

The Effect of Gingival Fibroblasts and Ultrasound on Orthodontically Induced  
Root Resorption in Beagle Dogs

by

Jacqueline Crossman

A thesis submitted in partial fulfillment of the requirements for the degree of

Master of Science

in

Medical Sciences – Oral Biology

University of Alberta

©Jacqueline Crossman, 2015

## **Abstract**

A favourable tooth crown-to-root ratio is required for supporting the tooth, but also for withstanding occlusal forces. This ratio is adversely affected when the tooth root is shortened. Orthodontically induced tooth root resorption is an unwanted side effect of orthodontic tooth movement. In severe cases, resorption of the tooth root apex progressing coronally results in tooth root shortening, which may lead to tooth loss. This type of root resorption is reported to occur in 40% of adults receiving orthodontic tooth movement where these patients had root shortening of 2.5 mm or more in at least one of their teeth. Orthodontically induced root resorption may even occur within 35 days of orthodontic treatment and even with only light forces.

Currently, no simple and reliable technique is available to repair the damage caused by orthodontically induced root resorption, therefore, a new method is needed that can regenerate the lost tooth root tissue. Low intensity pulsed ultrasound has been reported to enhance osteoblastic differentiation, increase proliferation, and induce osteogenic differentiation in cells. It has also been shown to enhance the repair of resorbed tooth roots in Beagle dogs.

Another treatment technique involved in periodontal repair (including alveolar bone and cementum) is stem cell therapy. Stem cells, and cells that have stem cell properties, that possibly could be used in periodontal repair, including periodontal ligament (PDL) stem cells, bone marrow stem cells, and gingival cells/fibroblasts, have shown promise in repairing periodontal defects, however, gingival cells/fibroblasts are more easily accessible and involve less donor site morbidity.

Previous to the current study, there is no study that had evaluated the effect of LIPUS and osteogenic induced gingival fibroblasts (OIGFs) on the repair of orthodontically induced root resorption. Therefore, the aim of the present study was to evaluate the effect of these treatment modalities (OIGFs and LIPUS) using histomorphometric and micro-computed tomography analyses.

The results of this study using histomorphometric analysis revealed that ultrasound and the combination of ultrasound and OIGFs were effective at increasing cementum thickness near the apex of the root ( $p < 0.05$ ). Also, ultrasound, OIGFs, and the combination of these two treatments increased periodontal ligament cellularity ( $p < 0.05$ ). However, there appeared to be no effect of these treatments on the width of the periodontal ligament ( $p > 0.05$ ). Using micro-computed tomographic analysis, it was shown that ultrasound, OIGFs, and the combination of the two treatments had an effect on reducing root resorption lacunae depth and volume ( $p < 0.05$ ), however, there was no effect on increasing tooth root length and reducing root resorption lacunae length ( $p > 0.05$ ).

In conclusion, using low intensity pulsed ultrasound and OIGFs, alone or in combination with each other, may have a promising effect on repairing damage caused by orthodontically induced root resorption. Additional studies that examine these treatments' effects on the inflammatory aspect of root resorption, employing a carefully separated multipotent gingival cells, and track/ label these cells to determine their incorporation into the tissues are required to fully understand their effect in this repair process.

## **Preface**

This thesis is an original work by Jacqueline Crossman. The research project, of which this thesis is a part, received research ethics approval from the University of Alberta Research Ethics Board, Project Name “New therapeutic techniques to improve dentofacial tissue repair and tissue engineering and Breeding Colony”, No. AUP00000248, October 28, 2014 (Approval Renewal Date).

## **Acknowledgements**

The research part of this thesis was supported by Qatar National Research Fund NPRP 09 - 557

- 3 – 144.

## **Table of Contents**

CHAPTER I: INTRODUCTION	1
I.I. Statement of Problem	2
I.II. Study Aim and Hypotheses	5
CHAPTER II: BACKGROUND AND LITERATURE REVIEW	6
II.I. Orthodontically Induced Root Resorption and Osteoclasts	7
II.II. Osteoblasts	9
II.III. Periodontal Repair and Stem Cells	10
II.IV. Low Intensity Pulsed Ultrasound	13
CHAPTER III: MATERIALS AND METHODS	16
III.I. Animals	17
III.II. Tooth Preparation and Orthodontic Tooth Movement	18
III.III. Gingival Cells	23
III.IV. Osteogenic Induction of Gingival Fibroblasts	24
III.V. Treatment Groups	25
III.VI. Tissue Preparation for Analysis	27

III.VII.	$\mu$ CT Scanning and Histology	27
III.VIII.	$\mu$ CT Analysis	29
III.IX.	Histomorphometric Analysis	33
III.X.	Statistical Analysis	36
CHAPTER IV: RESULTS		38
IV.I.	Flowcytometry and ALP Assay	39
IV.II.	Histology and Histomorphometric Analysis	40
IV.III.	$\mu$ CT Analysis	48
CHAPTER V: DISCUSSION		55
V.I.	Osteogenically Induced Gingival Fibroblasts	56
V.II.	Histomorphometric Analysis	59
V.III.	$\mu$ CT Analysis	68
V.IV.	Limitations	72
V.V.	Future Work	74
V.VI.	Conclusions	75
REFERENCES		77
APPENDIX		89

## **List of Abbreviations**

μCT: micro-computed tomography

3D: three dimensional

ALP: alkaline phosphatase

ANOVA: analysis of variance

bmp: bitmap

BMP-2: bone morphogenetic protein-2

BMPs: bone morphogenetic proteins

Cbfa1: core-binding factor alpha 1

CD11b: cluster designation/cluster of differentiation 11b

CD14: cluster designation/cluster of differentiation 14

CD19: cluster designation/cluster of differentiation 19

CD34: cluster designation/cluster of differentiation 34

CD73: cluster designation/cluster of differentiation 73

CD79α: cluster designation/cluster of differentiation 79-alpha

CD90: cluster designation/cluster of differentiation 90

CD105: cluster designation/cluster of differentiation 105

CEJ: cementoenamel junction

cN: centinewton

DMEM: Dulbecco's modified eagle's medium

EDTA: ethylenediaminetetraacetic acid

FITC: fluorescein isothiocyanate

GF(s): gingival fibroblast(s)

HEPES: hydroxyethyl piperazineethanesulfonic acid

HLA-DR: human leukocyte antigen-DR

HSLAS: health sciences laboratory animal services

IgGa: immunoglobulin Ga

IgGk1: immunoglobulin Gk1

IL-1: interleukin 1

IL-6: interleukin 6

ISCT: International Society for Cellular Therapy

kHz: kilohertz

LIPUS: low intensity pulsed ultrasound

MEM: minimal essential medium

MHC-II: class II major histocompatibility complex

MHz: megahertz

MSCs: mesenchymal stem cells

mW: milliwatt

OIGFs: osteogenic induced gingival fibroblasts

OIRR: orthodontically induced inflammatory root resorption

OI(T)RR: orthodontically induced (tooth) root resorption

OPG: osteoprotegerin

OPN: osteopontin

Osx: osterix

PDL: periodontal ligament

PE: phycoerythrin

PVS: polyvinyl siloxane

RANK: receptor activator of nuclear factor-kappaB

RANKL: receptor activator nuclear kappa-B ligand

ROI: region of interest

RT-PCR: reverse transcriptase polymerase chain reaction

Runx-2: runt-related transcription factor 2

SEM: standard error of the mean

SMRI: surgical-medical research institute

TNF-alpha: tumor necrosis factor-alpha

TRAP: tartrate-resistant alkaline phosphatase

## **List of Figures**

3-1	Dental bite block	19
3-2	Premolar crown preparation	19
3-3	PVS impression	19
3-4	Stone models and full crown wax ups with steel wires and brackets	20
3-5	Metal alloy crowns with attached tubes	20
3-6	NX3 Nexus® Third Generation dual cure permanent resin cement system	22
3-7	Digital calipers	23
3-8	Transosseous injection of OIGFs Dentsply™ X-Tip Intraosseous Anesthetic Delivery System, Pennsylvania.	26
3-9	Teeth sectioning at coronal, middle, and apical root levels	28
3-10	μCT slice showing tooth enamel (white)	29
3-11	μCT analysis showing root resorption lacunae (red arrow)	30
3-12	μCT analysis measuring root resorption volume using interpolated regions of interest	32
3-13	μCT analysis measuring root resorption volume using binary selection (SkyScan®)	32

3-14	<p>μCT analysis measuring root resorption volume using morphometry in CTAn (SkyScan®).</p>	33
3-15	<p>Histomorphometric analysis of cementum thickness (coloured lines)</p>	34
3-16	<p>Histomorphometric analysis of PDL thickness (coloured lines)</p>	35
3-17	<p>Histomorphometric analysis of PDL cell count</p>	36
4-1	<p>Immunophenotyping of canine gingival cells using flowcytometry with antibodies (CD11b, CD14, CD34, CD45, CD74, CD90, and CD105) to identify percentage of gated cells (%). FITC-conjugated Isotype-mouse IgGa1 and PE-conjugated Isotype-mouse IgGk1 were control antibodies</p>	39
4-2	<p>ALP assay showing ALP activity (absorbance level at 405nm) of canine gingival cells after four treatments – culture in medium without ultrasound, culture in medium with ultrasound, culture in osteogenic medium without ultrasound, and culture in osteogenic medium with ultrasound</p>	40
4-3	<p>Digital histologic images of cementum and periodontal ligament from each treatment group on the compression (A) and tension (B) sides of the tooth root at coronal (level 1), middle (level 2), and apical (level 3) root levels</p>	41

4-4	Cementum thickness ( $\mu\text{m}$ ) (mean $\pm$ SEM) in each treatment group  on the compression (A) and tension (B) sides of the tooth root at coronal  (level 1), middle (level 2), and apical (level 3) root levels	46
4-5	Periodontal ligament width ( $\mu\text{m}$ ) (mean $\pm$ SEM) in each treatment group  on the compression (A) and tension (B) sides of the tooth root at coronal  (level 1), middle (level 2), and apical (level 3) root levels	47
4-6	Periodontal ligament cell count (mean $\pm$ SEM) in each treatment group  on the compression (A) and tension (B) sides of the tooth root at coronal  (level 1), middle (level 2), and apical (level 3) root levels	48
4-7	$\mu\text{CT}$ reconstructed image of a tooth root with evidence of orthodontically  induced root resorption (red arrow)	49
4-8	Root length (mm) (mean $\pm$ SEM) as evaluated by $\mu\text{CT}$ analysis in each  treatment group	51
4-9	$\mu\text{CT}$ analysis of root resorption lacunae depth (mm) (mean $\pm$ SEM) in  each treatment group	52
4-10	$\mu\text{CT}$ analysis of root resorption lacunae length (mm) (mean $\pm$ SEM) in  each treatment group	53

4-11	$\mu$ CT analysis of root resorption lacunae volume ( $\text{mm}^3$ ) (mean $\pm$ SEM) in each treatment group	54
Appendix 1-1	Clinical signs checklist	89
Appendix 1-2	Pain Assessment In The Dog Scoring Sheet	90

**List of tables**

3-1	Number of premolars included in each treatment group	17
4-1	Cementum thickness ( $\mu\text{m}$ ) (mean $\pm$ SEM), PDL width ( $\mu\text{m}$ ) (mean $\pm$ SEM), and PDL cell count ( $\mu\text{m}$ ) (mean $\pm$ SEM) in each treatment group on the compression (A) and tension (B) sides of the tooth root at coronal (level 1), middle (level 2), and apical (level 3) root levels	43
4-2	Root lengths (mm) (mean $\pm$ SEM), root resorption lacunae depth (mm) (mean $\pm$ SEM), root resorption lacunae length (mm) (mean $\pm$ SEM), and root resorption lacunae volume ( $\text{mm}^3$ ) (mean $\pm$ SEM) in each treatment group	50

# **Chapter I: Introduction**

## **I.I. Statement of problem**

Orthodontically induced inflammatory tooth root resorption (OIIRR), also known as orthodontically induced root resorption (OIRR), is an unwanted and unavoidable result of orthodontic tooth movement (Brezniak and Wasserstein, 2002). There are three degrees of OIRR with respect to its severity. These are: cemental/surface resorption, dentinal/deep resorption, and circumferential apical resorption (Brezniak and Wasserstein, 2002). During cemental or surface resorption, only the outer cementum is resorbed. These outer layers are later fully regenerated or remodeled. The second degree of severity, dentinal resorption, involves the cementum and outer layers of dentin becoming resorbed. This process is usually repaired with cementum, however, the final shape of the root after repair may not be identical to its original contour. Finally, the third degree, circumferential apical root resorption, is the most severe, and is sometimes called severe root resorption. During this process, full resorption of hard tissue components of the apex of the root occurs. This type of OIRR results in shortening of the root (Brezniak and Wasserstein, 2002). When the root decreases in length, the crown-to-root ratio is adversely affected. Maintaining an optimal crown-to-root ratio is required in order to support the tooth and also to withstand occlusal forces (Cwyk et al., 1984).

A report on the prevalence of OIRR revealed that 40% of adults receiving orthodontic tooth movement had at least one of their teeth with 2.5 mm or greater of root resorption (Mirabella and Artun, 1995). This demonstrates that these patients had tooth roots shortened by 2.5 mm or more due to damage caused by severe OIRR. It has also been reported that OIRR may occur within as short of a period as 35 days of orthodontic treatment (Harry and Sims, 1982). This can even take place with orthodontic forces as light as 50 grams (Harry and Sims, 1982).

Currently, there is no treatment technique available to repair damage that has been caused by severe OIRR. Therefore, a new technique is needed that is able to regenerate the lost tooth root parts after OIRR has occurred.

Ultrasound is acoustic pressure waves that are transmitted through living tissues. It is frequently used as a therapeutic, operative, and diagnostic technique in medicine (Maylia and Nokes, 1999; Ziskin 1987; Dyson, 1985). Although the intensity applied in therapy ranges from 30 to 70,000 mW/cm<sup>2</sup>, operative and diagnostic ultrasound can range in intensity from 0.005 to 27,000,000 mW/cm<sup>2</sup> (Ritchie et al., 2013; Li et al., 2006). Many studies that have used low intensity pulsed ultrasound (LIPUS) in research and clinical application. Many researchers have tested its effect on different cells/tissues/organs using a frequency of 1.5 MHz repeating at 1 kHz with an intensity of 30 mW/cm<sup>2</sup> of the transducer's surface area, and it is relatively agreed that the optimal daily exposure of LIPUS is 20 min/day (Tanaka et al., 2015). Reports have evaluated the stimulatory effect of LIPUS on a variety of cell types, which include PDL cells (Harle et al., 2001b; Hu et al., 2014; Ikeda et al., 2009; Rita et al., 1999), cementoblastic cells (Dalla-Bona et al., 2006; Dalla-Bona et al., 2008; Inubushi et al., 2008; Rego et al., 2010), odontoblast-like cells (Scheven et al., 2009), muscular cells (Nagata et al., 2013), chondrocytes (Iwabuchi et al., 2014; Mukai et al., 2005; Schumann et al., 2006; Takeuchi et al., 2008), bone cells (Leung et al., 2004; Naruse et al., 2003), human alveolar mesenchymal stem cells (MSCs) (Lim et al., 2013), and synovial cells (Nakamura et al., 2010). Inubushi et al. (2008) reported that the use of LIPUS on periodontal ligament (PDL) cells enhanced the differentiation of these cells into cementoblast-like cells. LIPUS has also been shown to have a stimulatory effect on gingival cells (Mostafa et al., 2009; Shiraishi et al., 2011). LIPUS has been demonstrated to increase cellular proliferation in gingival fibroblasts (Doan et al., 1999) and to induce osteogenic differentiation of these

gingival cells (Mostafa et al, 2008). A more recent study showed that LIPUS enhances the repair of resorbed tooth roots in beagle dogs (Al-Daghreer et al., 2014).

Another possible treatment technique of lost periodontal and dental tissues is stem cell therapy. A variety of stem cells have been studied for their possible use in repair of periodontal defects (Kawaguchi et al., 2004; Yamada et al., 2006; Tobita et al., 2008). Human PDL stem cells and bone marrow stem cells have been shown to repair PDL defects in mice and rats (Seo et al., 2004) and in dogs (Kim et al., 2009). Another study reveals that PDL fibroblast-like cells have capability in preventing root resorption and inducing cementum formation in dogs (Dogan et al., 2002). Although current techniques that use these stem cells in periodontal repair have achieved preliminary successes, these studies suffer from significant drawbacks, such as donor site morbidity. Therefore, better sources of stem/progenitor cells are needed for PDL tissue repair and OIRR treatments.

An alternate type of multipotent cell that has shown promise in dental and periodontal repair is the gingival fibroblast (GF). This type of cell may be more easily accessible compared to other types of stem cells. Previous studies using GFs reveal that they can enhance vascularization *in vivo* (Mohammadi et al., 2007). Gingival fibroblasts have been able to be differentiated into osteogenic cells (Mostafa et al., 2008a). Osteogenic differentiation of GFs may be necessary in their promotion of repair of lost hard tissues. Alkaline phosphatase (ALP) is a widely recognized biochemical marker of an osteoblast phenotype (Sabokbar et al., 1994). ALP is an enzyme that catalyzes the hydrolysis of phosphate esters at an alkaline pH. It is responsible for the mineralization characteristic of osteogenic/osteoblast cells. The absence of osteogenic differentiation suggests that ALP activity and therefore mineralization activity would be low or

absent, which may show the necessity of this differentiation in re-establishing lost mineralized dental tissue.

## **I.II. Study aim and hypotheses**

There is no study that has evaluated the effect of LIPUS and osteogenic induced gingival fibroblasts (OIGFs) on repair of orthodontically induced root resorption. The aim of this present study was to analyze this possible effect of these two treatment modalities using histomorphometric analysis and micro-computed tomography analysis. The hypotheses of the present study were:

1. LIPUS and OIGFs will show more repair of the OIRR compared to the control group as evaluated by increased cementum thickness PDL cell count. The increased cementum thickness and PDL cell count would be greater in the LIPUS + OIGFs group compared to either the LIPUS group or the OIGFs group.
2. Tooth roots would be longer in the LIPUS group and the OIGFs group compared to the control group, and would be greater in the LIPUS + OIGFs group compared to either the LIPUS group or the OIGFs group
3. Root resorption lacunae length, depth, and volume would be greater in the LIPUS group and the OIGFs group compared to the control group, and would be greater in the LIPUS + OIGFs group compared to either the LIPUS group or the OIGFs group

## **Chapter II: Background and literature review**

## **II.I. Orthodontically induced root resorption and osteoclasts**

Orthodontically induced tooth root resorption is a pathological process that occurs during orthodontic tooth movement. Force application during orthodontic treatment induces a local process that includes all of the characteristics of an inflammatory reaction. These include rubor (redness), calor (heat), tumor (swelling), dolor (pain), and functio laesa (inhibited function). This inflammatory reaction is essential to tooth movement, and is the fundamental component behind the root resorption process. Since this type of root resorption involves such processes, it is more accurately termed orthodontically induced inflammatory root resorption (Brezniak and Wasserstein, 2002).

OIRR is part of the hyaline zone elimination process (Brezniak and Wasserstein, 2002). During orthodontic tooth movement, force application results in the over-compression of the PDL. Blood flow is retarded and stagnated in these pressure zones, which leads to sterile necrosis of soft tissues. Removal of such tissues begins at the periphery of this hyaline zone. Mononucleated and tartrate-resistant acid phosphatase (TRAP) negative cells initially access the root surface (Mavragani et al., 2004). These precursor clastic cells arise from pluripotent hemopoietic stem cells. Recruitment of such precursors involves a complex interaction between osteoblasts, stromal bone cells, and hemopoietic cells. However, the cellular and molecular mechanisms that occur during clastic cell formation are not fully known due to the lack of knowledge of the exact sequence of events that are involved during this process (Arana-Chavez and Bradaschia-Correa, 2009).

These precursor resorptive cells are likely activated by signals secreted by the sterile necrotic tissue (Brezniak and Wasserstein, 2002), but are also responsive to growth factors that are

secreted by various types of mesenchymal cells. Precursor clastic cells become multinucleated TRAP-positive cells without ruffled borders by fusion with other precursor clastic cells. The exact process involved in fusion of mononucleated precursor clastic cells is relatively unknown, however, the involvement of proteins and glycoconjugates of the plasma membrane in this process has been described (Arana-Chavez and Bradaschia-Correa, 2009). The activation of fused clastic cells is regulated by the activation of receptor activator nF-kB (RANK), which is expressed in the plasma membrane of fused clastic cells. The ligand of RANK (RANKL) is a soluble protein that is secreted by osteoblasts and also their precursors in bone. RANKL binds to RANK and then stimulates differentiation pathways in clastic cell precursors. After differentiation of these clastic cells, the resorptive cells remove the majority of necrotic PDL tissues and resorb the outer layer of adjacent root cementum (Mavragani et al., 2004), the cementoid, which is uncalcified cementum or precementum (Brezniak and Wasserstein, 2002). This damage to cementoid tissue exposes the underlying highly dense mineralized cementum. However, it may be possible that the orthodontic force applied may directly damage the cementoid tissue, resulting in its inevitable removal by resorptive cells (Brezniak and Wasserstein, 2002). Clastic cell activity is regulated by osteoprotegerin (OPG), which is a soluble protein also secreted by osteoblasts. This protein binds to RANK preventing RANKL from binding to RANK, and therefore inhibiting genesis of clastic cells (Arana-Chavez and Bradaschia-Correa, 2009).

The root resorption process continues until either the force level decreases or the hyaline tissue is no longer present. Removal of hyaline tissue and resorption of tooth root cementum is a method that results in a pressure decrease. Root resorption lacunae, which are small and large pits that form on the surface of the tooth root as a result of root resorptive activity, increase the surface

area of the root, thereby decreasing applied pressure exerted through orthodontic force application. Decompression therefore reverses this process, and cementum may be repaired to a certain degree (Brezniak and Wasserstein, 2002).

## **II.II. Osteoblasts**

After resorptive activity occurs, the remodeling process takes place through osteoblast activity. Osteoblasts are mononucleated cells that are derived from mesenchymal stem cells. Prior to their commitment as osteoblasts, these cells can also differentiate into other mesenchymal cells such as fibroblasts, chondrocytes, myoblasts, and bone marrow stromal cells including adipocytes. Regulation of the expression of osteoblast-specific genes, such as *Cbfa1* (core-binding factor  $\alpha 1$ ), *Runx-2*, and *Osx* (osterix), is responsible for the commitment of multipotent mesenchymal cells to osteoblastic lineage and for osteoblast differentiation (Neve et al., 2011).

Osteoblast commitment, differentiation, and growth are also controlled by several local and systemic factors, such as bone morphogenetic proteins (BMPs). One type of the BMPs is bone morphogenetic protein-2 (BMP-2), which has been shown to be able to induce immature cells to differentiate into osteoblasts. In one study that looked at the effect of BMP-2 on beagle dog tooth roots, it was shown that BMP-2 significantly increase cementum-like tissue formation in tooth defects created, and that BMP-2 decreased epithelial down-growth (Miyaji et al., 2010).

Osteoblast precursor cells that undergo proliferation and differentiation into pre-osteoblasts are unable to deposit bone matrix, however, they are still capable to proliferate. During this phase, BMP-2 plays a role in increasing alkaline phosphatase activity, evidence of mineralization by osteoblasts (Neve et al., 2011).

After the arrest of growth, selective expression of genes occurs, which results in characterization of differentiated osteoblast phenotype. Active bone-matrix-secreting osteoblasts are provided with regions of plasma membrane specialized in trafficking and secretion of vesicles that deposit bone matrix. These cells use tight junctions for communication (Neve et al., 2011).

Bone remodelling is a constant process in which osteoblasts play an essential role not only in deposition of bone matrix, but also in regulation of osteoclast activity through osteoblast secretion of bone matrix proteins such as osteopontin and bone sialoprotein (Neve et al., 2011), and also OPG and RANKL (Arana-Chavez and Bradaschia-Correa, 2009) . After resorption has occurred, osteoblasts migrate into resorption lacunae created by osteoclasts, and synthesize new un-mineralized bone matrix that fills resorption lacunae and becomes mineralized (Neve et al., 2011).

### **II.III. Periodontal repair and stem cells**

Periodontal disease is a chronic inflammatory condition of the periodontium, which is a complex organ consisting of two soft connective tissues (gingiva and periodontal ligament) and two hard connective tissues (cementum and alveolar bone) (Maeda et al., 2011; Lin et al., 2008). If periodontal disease is left untreated, it may result in compromised dentition that includes premature tooth loss (Silvério et al., 2008; Lin et al., 2008). The ultimate goal of periodontal therapy and repair is the reconstruction of gingival connective tissue, cementum, alveolar bone, and PDL (Garrett, 1996. Lin et al., 2008). Cementum is avascular, bone-like connective tissue that lines the tooth root. Cementoblasts, which are functionally similar to osteoblasts, are usually contained within lacunae that are formed during resorption. Cementum is responsible for

anchoring PDL fibre bundles to the tooth root. PDL, on the other hand, is highly specialized fibrous connective tissue that is present between the cementum and the bone. It is highly vascularized tissue and contains osteoblasts, osteoclasts, and cementoblasts, which although are contained within the PDL, are functionally associated with bone and cementum (Nanci and Bosshardt, 2006; Lin et al., 2008).

Current treatment regenerative approaches need to include healing events in an ordered and programmed sequence. Appropriate progenitor cells must first migrate or be introduced to the area where repair is to occur. These cells must proliferate and mature into the tissue components of function periodontal attachment apparatus. The success of such proliferation, migration (or deposition), and maturation of these cells depends on the availability of growth factors.

Progenitor cells of particular interest in periodontal repair are osteoblasts, cementoblasts, and fibroblasts, all of which are responsible for restoration of lost periodontal tissues. (Lin et al., 2008)

Stem cells have been introduced as potential clinical therapy in periodontal repair. A variety of stem cell populations, including bone marrow-derived mesenchymal stem cells (MSCs) and dental-derived mesenchymal stem cells, have been considered for used in this therapy. By definition, a stem cell refers to a clonogenic and relatively undifferentiated cell that is capable of self-renewal and multi-lineage differentiation. Dental-tissue-derived mesenchymal stem cell-like populations are among other isolated and characterized stem cells that reside in specialized tissues. Initially, dental MSCs were isolated from human pulp tissue. Subsequently, stem cells from exfoliated deciduous teeth, PDL stem cells, and stem cells from apical papilla were also isolated and characterized. More recent studies have also isolated and characterized stem cells from the dental follicle and gingiva. Although this isolation and characterization of these cells

has occurred, the developmental relationships, growth rate, and gene and protein expressions of these cells are relatively unknown. (Lin et al., 2008)

Human PDL stem cells and bone marrow stem cells have been used in studies to demonstrate the capability of these cells to regenerate a variety of periodontal defects in mice, rats, and dogs (Kawaguchi et al., 2004; Yamada et al., 2006; Tobita et al., 2008). Human PDL fibroblast-like cells have been shown to prevent root resorption and to induce cementum formation also in dogs (Dogan et al., 2002). Although these studies using stem cells in periodontal repair have achieved preliminary successes, they may suffer from significant drawbacks such as donor site morbidity. Therefore, better sources of stem cells are needed for PDL tissue repair, and also for OIRR treatments.

More recent studies have focused on the use of gingival fibroblasts (GFs), which show promise in dental and PDL repair due their easier accessibility. GFs have been shown to enhance gingival attachment in humans (Mohammadi et al., 2007). In this study GFs were obtained from attached gingiva and were cultured. The GFs were incorporated into a tissue-engineered mucosal graft implanted into patients with insufficient attached gingiva. After three months of healing, the GFs group showed a significantly greater amount of attached gingiva compared to the control group.

Another study investigated the potential of gingival cells inhibiting osteoclast activity, this inhibition being a property of osteoblasts (de Vries et al., 2006). This study revealed that although these cells are associated with other factors in the formation of osteoclast-like cells, they more importantly play a role in preventing bone resorption that results from osteoclast activity. A further study showed the possibility to differentiate gingival fibroblast cells into osteogenic phenotype (Mostafa et al., 2008a). Osteogenic and osteoblast cells express high

activity of ALP, which is a common marker of these types of cells (Sabokbar et al., 1994). ALP activity indicates mineralization potential, which is necessary for these cells to repair lost hard tissues. Osteogenically induced gingival cells/fibroblasts may have better potential in re-establishing dental tissues that have been damaged than gingival cells without osteogenic differentiation based on ALP activity and mineralization.

An additional study researched gingival cellular role in dental papilla reconstruction in humans using an injection technique. This study showed the efficacy of an autologous gingival fibroblast injection technique at early stages of healing of interproximal papilla defects (McGuire and Scheyer, 2007).

These studies suggest that gingival fibroblasts may be used in a promising technique of periodontal repair and more specifically in repair of damage caused by OIRR.

#### **II.IV. Low intensity pulsed ultrasound**

Another technique that has been studied regarding periodontal repair is low intensity pulsed ultrasound (LIPUS). LIPUS is pressure waves that are at frequencies above the limit of human hearing and that can promote tissue healing (Al-Daghreer et al., 2014; Azuma et al., 2001; Chapman et al., 1980; Chen et al., 2003; Claes and Willie, 2007). Ultrasound is used widely in medicine as a therapeutic, diagnostic, and operative tool (Maylia and Nokes, 1999; Ziskin, 1987; Dyson, 1985).

Although the exact biological mechanisms that are involved in tissue repair during LIPUS application are relatively unknown, it is suspected that the anabolic effect of LIPUS are caused

by mechanical stress, which impacts the cell plasma membrane, focal adhesion, and cytoskeleton, and then triggers intracellular signal transduction followed by gene transcription (Kanbe et al., 2009; Kokubu et al., 1999; Ren et al., 2013; Saito et al., 2004). Through these biological mechanisms, LIPUS has been used in bone repair, bone fracture healing acceleration, and osteogenesis enhancement at the distraction site (Azuma et al., 2001; Claes and Willie, 2007; Dyson et al., 1968; Dyson and Brookes, 1983; El-Bialy et al., 2002; El-Bialy et al., 2008; Erdogan et al., 2006; Abramovich, 1970; Heckman et al., 1994; Tsai et al., 1992; Warden et al., 2000). It has also been reported that LIPUS is effective in stimulating angiogenesis during wound healing (Young and Dyson, 1990). Other studies show that therapeutic ultrasound stimulates the expression of proteins such as OPN and bone sialoprotein. This effect has been shown to be dose dependent (Harle et al., 2001b; Cheung et al., 2011). Further studies demonstrated the anti-inflammatory action of ultrasound (Iashchenko et al., 1994; Nakamura et al., 2011; Nakamura et al., 2010).

In another study, it was demonstrated that LIPUS regulated osteoclast differentiation through the OPG/RANKL ratio. This study used LIPUS intensities of 100 and 150 mW/cm<sup>2</sup>. LIPUS was applied to tooth roots in rats undergoing orthodontic tooth movement. After these treatments, it was reported that osteoclast numbers and activity decreased and the OPG/RANKL expression ratios increased in the LIPUS-treated groups (Liu et al., 2012).

Another study compared the effect of different ultrasound intensities on cementoblasts. This study reported that an intensity of 150 mW/cm<sup>2</sup> significantly increased alkaline phosphatase activity, which has an essential function in the mineralization process by osteoblasts. Although this intensity may be most effective in stimulating cementoblasts *in vitro*, it was suspected that

this intensity may be harmful to cells *in vivo*, therefore additional investigation is necessary to determine the optimal LIPUS intensity (Dalla-Bona et al., 2006).

Current studies are demonstrating the possible future clinical application of LIPUS in minimizing OIRR. In one study, LIPUS was used to heal orthodontically induced root resorption in patients. It was reported in this study that LIPUS minimized the effect of OIRR by accelerating healing of the resorption by reparative cementum during simultaneous tooth movement and daily LIPUS application (El-Bialy et al., 2004).

## **Chapter III: Materials and methods**

### III.I. Animals

This research was approved by the University of Alberta Animal Research Ethics Committee. Seven beagle dogs were obtained through HSLAS at the University of Alberta and ordered from Marshall BioResources, North America. The average age of the dogs upon the start of the study was 1 year-7 months  $\pm$  8 days. The sample size was calculated in combination with another study in order to obtain a statistical power of 0.80. For each dog, third and fourth premolars on right and left sides of the mandible and maxilla were included in this study. This resulted in a total of 56 premolars. Each premolar received orthodontic tooth movement for four weeks, and then was randomly assigned to one of five treatment groups. These treatment groups are included in Table 3-1.

Table 3-1: Number of premolars included in each treatment group.

<b>Treatment Groups</b>	<b>Sample Size (Number of premolars)</b>
<b>Control (No treatment)</b>	6
<b>LIPUS</b>	5
<b>OIGFs</b>	6
<b>BMP-2</b>	5
<b>OIGFs + LIPUS</b>	6

Dogs were chosen as the preferred animal model in this study because the teeth physiology of dogs is reasonably close to that of humans, dogs have clinically relevant tooth size and tooth configuration, dogs are significantly easier to handle during postoperative management. Also, they have PDL relatively similar to that of humans, and they are subjects of extensive published

research experience particularly in the evaluation of different PDL repair treatments (Lee et al., 2010; Ikai et al., 2008; Sakallioğlu et al., 2004).

Upon the arrival of the dogs, they were isolated in an off-campus facility and were treated for Giardia using Flagyl. After this treatment, the animals were housed in the Dentistry/Pharmacy building animal facility under normal conditions and were determined to be physiologically similar at baseline.

### **III.II. Tooth preparation and orthodontic tooth movement**

To begin preparation of the teeth for orthodontic tooth movement, each dog was premedicated with a sedative and antiemetic (Acepromazine/SubQ/0.05 mg/kg), an analgesic (Hydromorphone/SubQ/0.1 mg/kg), and a muscarinic anticholinergic drug (Glycopyrrolate/SubQ/0.01 mg/kg). The dogs were then transferred to the Surgical Medical Research Institute (SMRI) at the University of Alberta. The animals were placed and secured on a heated surgical table and were intubated for the administration of the inhalation anesthesia. The dogs' mouths were held open using an adult sized bite block (Figure 3-1). Full crown preparation on the premolars was started using a high speed hand piece operating on NSK Mio Coreless Micromotor System using a tapered diamond bur cooled with saline (Figure 3-2). After full crown preparation, the premolars were cleaned and dried using water and gauze. This prepared the teeth for impression using plastic trays loaded with PVS. The tray was placed on the prepared premolars and held firmly using finger support for a total of five minutes. The tray was removed and the impression was evaluated for any defects or bubbles (Figure 3-3).



Figure 3-1: Dental bite block.



Figure 3-2: Premolar crown preparation.

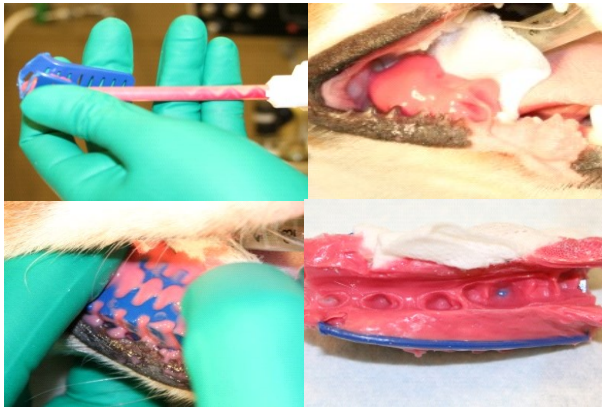


Figure 3-3: PVS impression.

After the oral cavity was cleared of impression materials and gauze, inhalation anesthesia was discontinued and the dogs were maintained on the table until normal breathing was restored.

Then, the dogs were transferred to recovery kennels.

A full crown wax up was completed for the third and fourth premolars on stone models that were poured out of the impressions (Figure 3-4). To prepare orthodontic appliances, GAC

DENTSPLY 0.022" x 0.28" bondable molar tubes were glued on the buccal surfaces of the

crowns of the premolar wax ups with straight 0.021” x 0.025” 3M stainless steel wires in the tube bracket slots to hold the tubes in the same vertical and horizontal orientation. This maintained pure bodily movements of the third and fourth premolars, mesially and distally, respectively. The wax ups and the attached tubes were then invested into dental investment materials. The crowns were casted into low fusing metal alloy and the wax was burned out (Figure 3-5). The crowns were finished and polished and the fitting surfaces were sandblasted with aluminum oxide particles.



Figure 3-4: Stone models and full crown wax ups with steel wires and brackets.



Figure 3-5: Metal alloy crowns with attached tubes.

The dogs were premedicated with a sedative and antiemetic (Acepromazine/SubQ/0.05 mg/kg), an analgesic (Hydromorphone/SubQ/0.1 mg/kg), and a muscarinic anticholinergic drug (Glycopyrrolate/SubQ/0.01 mg/kg), and then again transferred to the SMRI. The animals were placed and secured on a heated surgical table and then intubated for the administration of inhalation anesthesia. The mouths were kept in the open position using an adult sized bite block and the prepared teeth were cleaned using pumice and rubber cups and then cleaned with water. The teeth were dried and the crowns were tried on to check for their fitting. To cement the crowns to the premolars, the NX3 Nexus® Third Generation dual cure permanent resin cement system was used (Figure 3-6). The OptiBond All-In-One adhesive system was employed using the following steps that were supplied by OptiBond:

1. Thoroughly clean the preparations (pumice and prophylaxis cup). Wash thoroughly with water spray and air dry. Do not desiccate.
2. Using the disposable applicator brush, apply a generous amount of OptiBond All-In-One adhesive to the enamel/dentin surface. Scrub the surface with a brushing motion for 20 seconds.
3. Apply a second application of OptiBond All-In-One adhesive with a brushing motion for 20 seconds.
4. Dry the adhesive with gentle air first and then with medium air for at least 5 seconds with oil-free air.
5. Light-cure for 10 seconds.



Figure 3-6: NX3 Nexus® Third Generation dual cure permanent resin cement system.

The cement was removed using plastic dental instruments and dental floss. The mesiodistal dimensions of the crowns on each side (for maxilla and mandible) were measured using digital calipers (Figure 3-7). A piece of straight 0.021” x 0.025” 3M stainless steel wire was inserted into the attachment tube with an open coil spring that was compressed between the two tubes (on third and fourth premolars) in order to deliver a force of 100 cN per appliance, which was measured with a force gauge. The wires were bent on the mesial and distal ends in order to prevent its displacement. The opposing teeth were reduced using a diamond bur to remove any occlusal interference with the new crowns.



Figure 3-7: Digital calipers.

Postoperatively, the dogs were assessed twice on the day of operation and then daily for the next four days. The animals were assessed for clinical signs using a Clinical Signs Checklist (Appendix 1-1) and also for pain using a Pain Assessment In The Dog Pain Scoring Sheet (Appendix 1-2).

Orthodontic tooth movement was continued for a total of four weeks. Each week the coil springs were evaluated and re-adjusted in order to maintain a force level of 100 cN.

### **III.III. Gingival cells**

To isolate gingival cells/fibroblasts from each dog, interdental papilla from each third and fourth premolar was excised. This procedure was performed concurrently with orthodontic tooth movement in the dogs. The papilla was immersed in biopsy medium (Dulbecco's Modified Eagle's medium [DMEM], 100 units/mL penicillin, and 100  $\mu$ g/mL streptomycin). Then, these tissues were cut into smaller pieces, dispersed on slides, and placed in culture plates with basic medium (DMEM with 10% fetal bovine serum, 100 units/mL penicillin, and 100 $\mu$ g/mL streptomycin). The culture plates were incubated at 37°C in a humidified atmosphere. Gingival

cells surrounding the tissue explants became confluent at 2-3 weeks. These cells were removed using a solution of 0.08% trypsin and 24% ethylenediaminetetraacetic acid (EDTA), and then were transferred into culture flasks (De Vasconcellos et al., 2006).

A concurrent study obtained some of the canine gingival cells in order to use them in identification of a variety of mesenchymal stem cell markers. This study used flowcytometry to determine the multipotency of the cells obtained for this study (Figure 4-1). The antibodies that corresponded to cell surface markers employed in flowcytometry were CD11b, CD14, CD34, CD45, CD73, CD90, and CD105 (Dominici et al., 2006). Prior to stem cell marker identification, these cells were exposed to LIPUS treatment for a total of 20 minutes for one day. The intensity used was  $30 \text{ mW/cm}^2$ , and the ultrasound pulsed at 1.5 MHz and repeated at a frequency of 1 KHz. A total of 10,000 labeled cells were acquired and analyzed by flowcytometry and corresponding software.

#### **III.IV. Osteogenic induction of gingival fibroblasts**

The cultured gingival cells were then transferred to 48-well plates at a density of  $2.5 \times 10^3$  cells/well. The cells/fibroblasts were treated with osteogenic medium (basic medium, 10 mM  $\beta$ -glycerophosphate, 50 mg/L ascorbic acid, and 0.1  $\mu\text{M}$  dexamethasone) and received LIPUS treatment for 20 min/day for a total of four weeks using an incident intensity of  $30 \text{ mW/cm}^2$  of the transducer's surface (2.5 cm transducer). This procedure was previously described in the protocol of El-Bialy et al (2004). This procedure induced GFs to osteogenic differentiation, producing osteogenic induced gingival fibroblasts (OIGFs). To confirm osteogenic induction of these gingival fibroblasts, an alkaline phosphatase (ALP) assay was performed in a subsequent

study (Figure 4-2). ALP is considered an early marker for osteoblast and osteogenic differentiation (Mostafa et al., 2009; Leung et al., 2004; Yoon et al., 2009). The gingival fibroblasts (GFs) were cultured in two different media – alpha medium and osteogenic medium. Alpha control medium was composed of alpha MEM (450mL), fetal bovine serum (50mL), penicillin/streptomycin (50mL), and HEPES (10mmol). The osteogenic medium consisted of DMEM (450mL), fetal bovine serum (50mL), dexamethasone (10nM), B-Glycerophosphate (10mmol), ascorbic acid (50mg/mL), HEPES (10mmol), and penicillin/streptomycin (5mL). The GFs that were cultured in the alpha medium were divided into two groups. One group received LIPUS treatment for 20min/day for a total of 28 days, and the other group did not receive any treatment. The GFs that were grown in osteogenic medium were also divided in two groups – one group receiving LIPUS treatment, and the other group receiving no treatment. The absorbance (maximum slope) was recorded at 405nm for each group.

### **III.V. Treatment groups**

After four weeks of orthodontic tooth movement, treatments were completed on each third and fourth premolar according to the random treatment assignment mentioned above. The LIPUS group received LIPUS treatment for 20min/day for four weeks according to published protocol (El-Bialy et al., 2004). Each premolar in the OIGFs group received a single injection of OIGFs. One half millilitre of OIGFs (in DMEM) was injected transosseously (Dentsply™ X-Tip Intraosseous Anesthetic Delivery System, Pennsylvania) through the buccal plate of bone into the PDL near the apex of the roots (Figure 3-8). A single injection per premolar was employed. This injection was completed after the four weeks of tooth movement. The injection was

performed using a 30-gauge needle and the concentration of cells was  $2 \times 10^5$  cells/mL of DMEM. The viability of OIGFs after delivery through needle was checked before the actual injection of cells into each dog's PDL was performed. Each of these dogs received OIGFs injection using cells obtained from the same dog. The BMP-2 group (positive control group) received a local injection of BMP-2, which was achieved by conjugating BMP-2 in poly-D,L-lactic acid-polyethylene glycol polymeric delivery system as outlined by Saito et al (2003). The BMP-2 injection was implemented after the four weeks of orthodontic tooth movement. The OIGFs+LIPUS group received a combination of these two treatments. The control group received no additional treatment after four weeks of tooth movement with the exception of a single injection of DMEM without cells into the periapical area. This group was considered to be the negative control group.

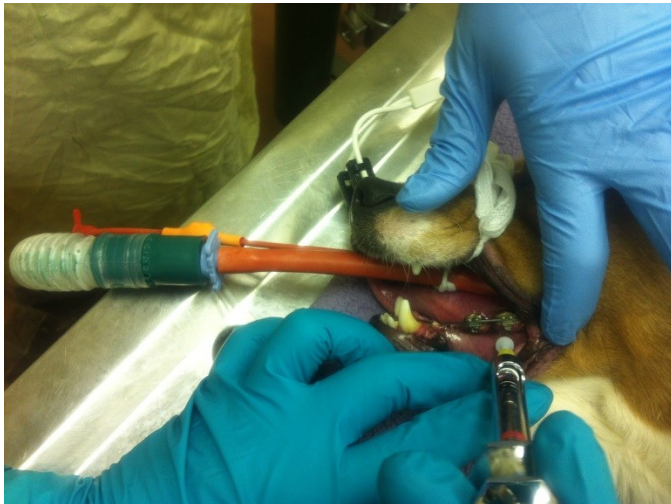


Figure 3-8: Transosseous injection of OIGFs (Dentsply™ X-Tip Intraosseous Anesthetic Delivery System, Pennsylvania).

### **III.VI. Tissue preparation for analysis**

After the four weeks of assigned treatments that took place after the orthodontic tooth movement, the animals were prepared for euthanasia by placing a 22-gauge catheter into the right cephalic vein and injected with DOMITOR® (medetomidine hydrochloride) (0.25 mg/kg IM) and then with 2-3 mL/4.5 kg of Euthanyl. Clinical death was confirmed by evaluating the vital signs.

The mandibles and maxillae of each dog were dissected and sectioned into blocks using a bone saw. Each block contained the third and fourth premolars with their supporting alveolar bone. The samples were stored into freshly prepared 4% paraformaldehyde in labeled containers.

### **III.VII. $\mu$ CT scanning and histology**

To perform micro-computed tomography ( $\mu$ CT) scanning, the samples were air dried for 30min prior to scanning. The samples were scanned in a SkyScan® 1076 MicroCT scanner and associated software (Version 2.6.0) at a resolution of 9 $\mu$ m using an x-ray source potential of 100 kV, an amperage of 100  $\mu$ A, and a power of 10W. The aluminum filter thickness was 1.0mm, and the scans averaged three times. The scanned images were reconstructed using NRecon© (Version 1.4.4) from SkyScan®. The images were then reconstructed selecting the tooth and associated PDL and bone as the Region of Interest (ROI), and under the following parameters: No Smoothing; Post Alignment (-0.5); Ring Artifact (6); beam hardening (25%); Output option: min. -867.1 Hounsfield units, max. 580.7 Hounsfield units. The reconstructed files were saved in an 8-bit \*.bmp format.

When  $\mu$ CT scanning was completed, the tissue blocks were rinsed in saline, fixed in 10% formalin, rinsed overnight in cold tap water, and then demineralized in 10% formic acid solution. The blocks were then washed with water and then decalcified in EDTA for 10 days. Serial sections that were 7 $\mu$ m in thickness were cut in the buccolingual plane throughout the entire mesiodistal extension of the teeth. These sections were made at three locations along the tooth root – at the coronal level near the crown, at the middle level of the root, and at the apical level near the apex of the root (Figure 3-9). These sections from each level were then mounted onto slides and deparaffinised by soaking them twice in fresh xylene for 10 min each time. The sections were stained with hematoxylin and eosin for analysis.<sup>1</sup>

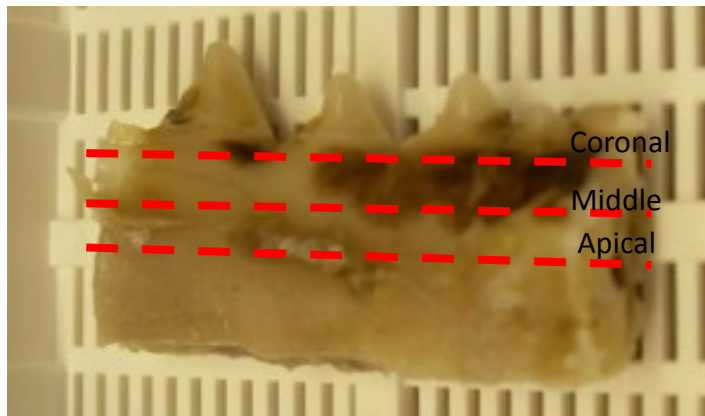


Figure 3-9: Teeth sectioning at coronal, middle, and apical root levels.

---

<sup>1</sup> The research materials and methods up to section III.VIII. were performed by another research team. The materials and methods continuing were performed by the author.

### III.VIII. $\mu$ CT analysis

Using  $\mu$ CT analysis, the tooth root lengths were first measured. The selected reconstructed file in the program CTAn (SkyScan®) was opened. The cementoenamel junction (CEJ) was located on the tooth in the raw images (Figure 3-10). This was performed by starting from the crown of the tooth and moving apically. The root length measurement was started at the next slice apical to the CEJ, where no enamel was evident on the slice. The slice location (in mm) was noted at the CEJ. After this, the assessor moved down apically through the slices until the first slice that no longer contained any image of the tooth root apex. This slice location (in mm) was noted. To calculate the entire root length these two slice locations were subtracted from each resulting in a root length measured in mm. This process was repeated for each tooth root. One hundred and one roots in total were available for analysis.

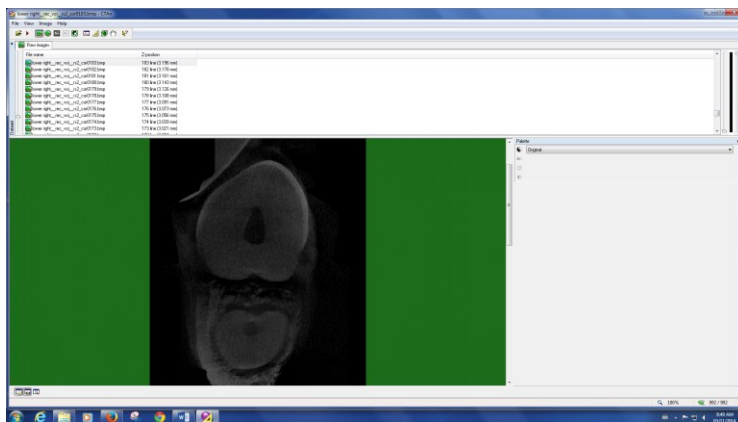


Figure 3-10:  $\mu$ CT slice showing tooth enamel (white).

Next, the length and depth of each resorption lacuna and the number of resorption lacunae was measured. The assessor began analysis at the CEJ, and began moving apically through the slices until a resorption lacuna (pit) was evident (Figure 3-11). The assessor noted when this resorption lacuna began and when it ended. The difference between these two measurements was used to calculate the length of the root resorption lacuna. To measure the depth of the lacuna, the slice with the deepest penetration of resorption was located. A line was drawn from the tooth surface inside the lacuna to the imaginary circumference of the tooth root. This line length was recorded. This process was continued for each resorption lacuna throughout the length of each tooth root (Table 4-2; Figure 4-8; Figure 4-9).

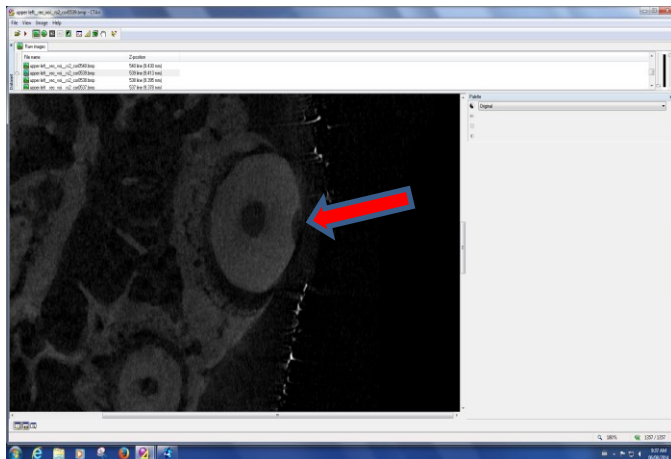


Figure 3-11:  $\mu$ CT analysis showing root resorption lacunae (red arrow).

To measure the volume of each root resorption lacuna, CTAn was employed again. The reconstructed image was again opened. First, the CEJ was located on the tooth root. Beginning at this slice, the assessor scrolled through the slices until the first resorption lacuna was evident.

The slice previous to that which contained first evidence of a lacuna was selected as the bottom of selection by right-clicking and selecting “Set the Bottom of Selection”. The assessor then moved apically through the slices until the slice immediately after the image that contained evidence of resorption lacuna. This slice was chosen as the top of selection by right-clicking and selecting “Set the Top of Selection”. Next, “Regions of Interest” was selected from the tool bar. Polygonal ROI was chosen from “Interpolated ROI” in order to measure the area of the lacuna in each slice. Nodes were added where needed in order to draw along the circumference of tooth root in the selected area where a lacuna was observed. The remaining area of the ROI was extended in order to cover an area greater than that of the lacuna at its deepest point (Figure 3-12). This created ROI was copied and pasted every 5-10 slices and adjusted depending on the depth and length of the lacuna. In “Binary Selection”, the greyscale indices were adjusted in the “From Image” tab in order to obtain an image of the tooth root that had the least number of black pixels while maintaining enough pixels to create a smooth circumference of the tooth root and perimeter of the resorption lacuna (Figure 3-13). The indices usually chosen were 30-40 on the bottom and 160 on the top. These indices varied depending on the quality of the image. In “Morphometry”, 3D Analysis was selected (Figure 3-14). The images were saved and then saved again by clicking “Save Results”. These saving options created excel spreadsheets containing data of tissue and bone volume. Tissue volume indicated the total tissue volume in the selected ROIs, and the bone volume represented the hard tissue volume (ie. Tooth root volume). To calculate the volume of the resorption lacuna, the bone volume was subtracted from the tissue volume, which resulted in soft tissue volume or empty space measurements and was equivalent to lacuna volume measurements. This process was continued until each root resorption lacunae volume was measured (Table 4-2; Figure 4-10).

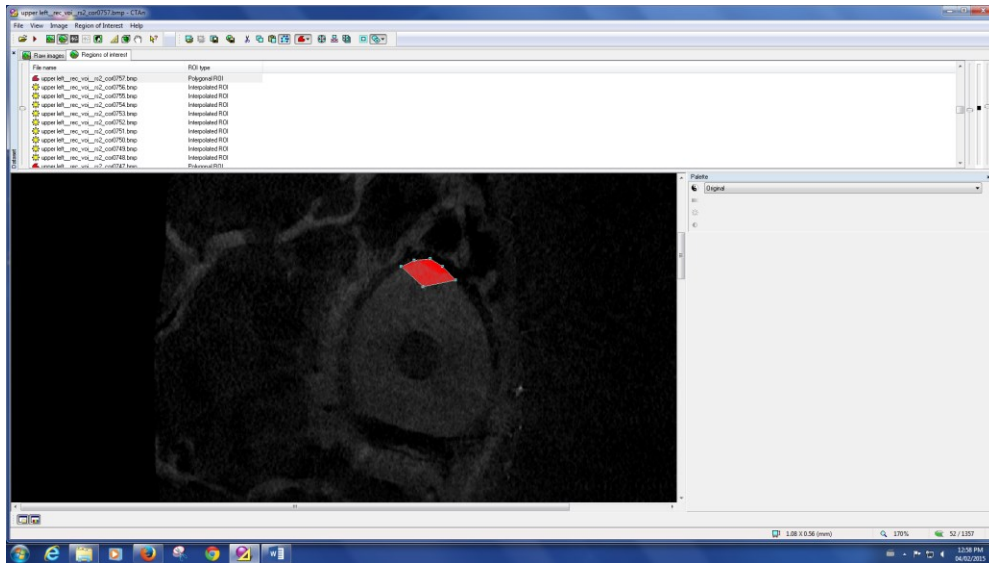


Figure 3-12:  $\mu$ CT analysis measuring root resorption volume using interpolated regions of interest.

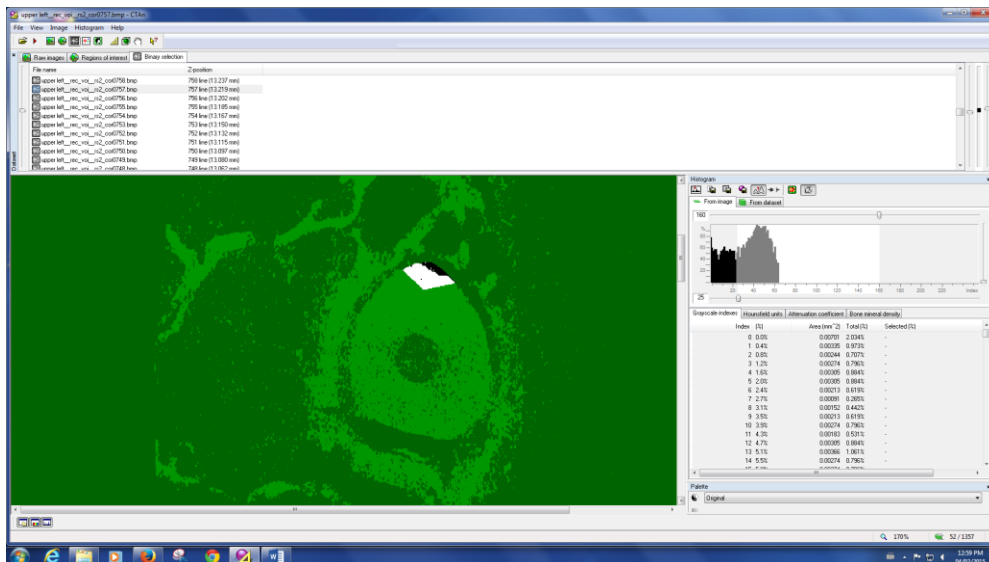


Figure 3-13:  $\mu$ CT analysis measuring root resorption volume using binary selection (SkyScan®).

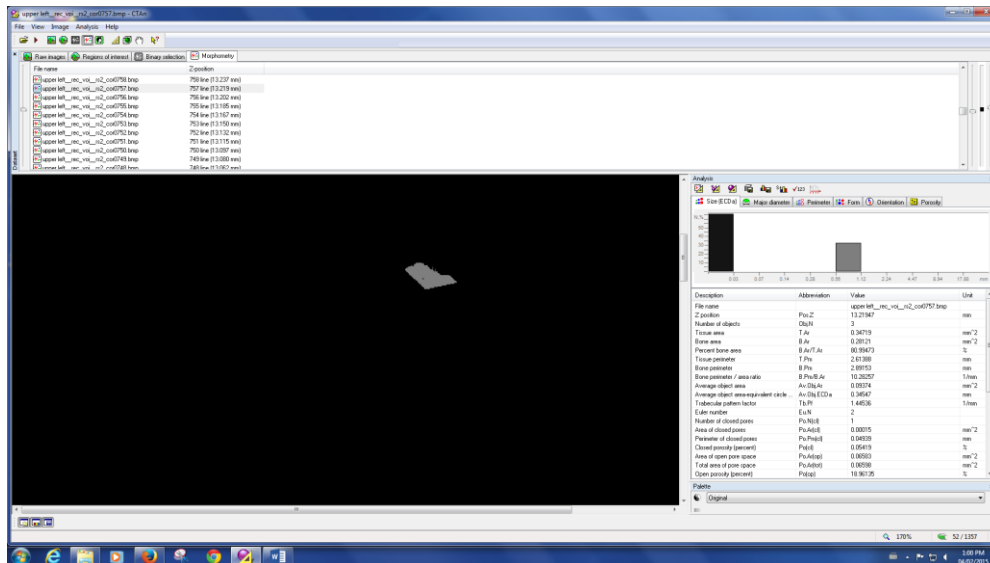


Figure 3-14:  $\mu$ CT analysis measuring root resorption volume morphometry in CTAn (SkyScan®).

### III.IX. Histomorphometric analysis

Histomorphometric analysis was then performed using the computer software MetaMorph Offline (Molecular Devices LLC, California). First, each slide was analyzed by light microscopy and digital images were created using this microscopy and digital camera at 40X magnification. Images were created for the distal and mesial sides of the tooth root in the mandible and each image included dentin, cementum, PDL, and bone from the designated side of the tooth root (Figure 4-3). Fifty-six roots in total were included in histomorphometric analysis.

To perform cementum thickness measurements, pre-set calibration files were selected for 40X magnification. One of the created digital images was opened, and using the line tool available in the tool bar, six lines were drawn over the appropriate tissue's layer from the top to the bottom of the layer (Figure 3-15). These lines were drawn parallel to and equally distributed from each

other as accurately as possible. An excel file was opened simultaneously and minimized. In MetaMorph, “Measure” was selected, followed by clicking “Region Measurements”. The data from the measurements were then displayed. “Open Log” was selected, and the Log File was named indicating details of the side of the root, the root level, and from which tooth root, which premolar, which side of mandible, and which dog the sample was. This file was saved, and the application name to which the data was exported was selected by only clicking “OK”. “F9: Log Data” was selected in order to transfer the measured data to the excel file that was previously opened. The first excel sheet opened for each dog became the master excel spread sheet. Subsequent cementum measurements were copied from their excel spreadsheets and pasted into the master sheet.

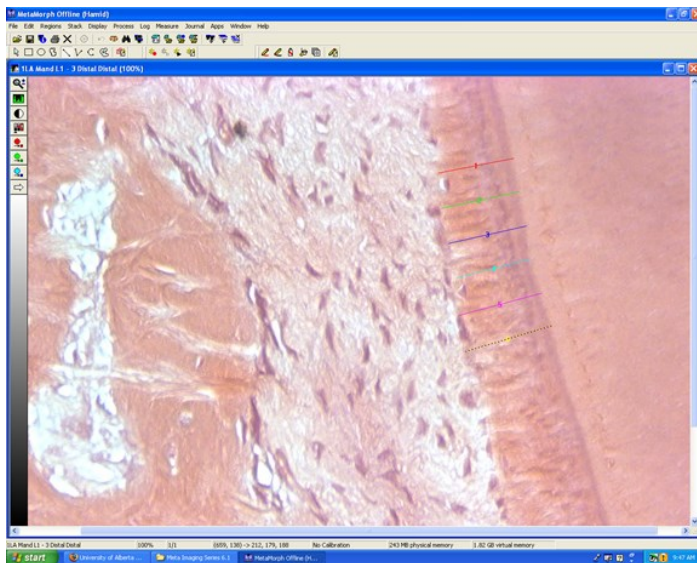


Figure 3-15: Histomorphometric analysis of cementum thickness (coloured lines).

PDL width measurements were performed in an identical manner (Figure 3-16).

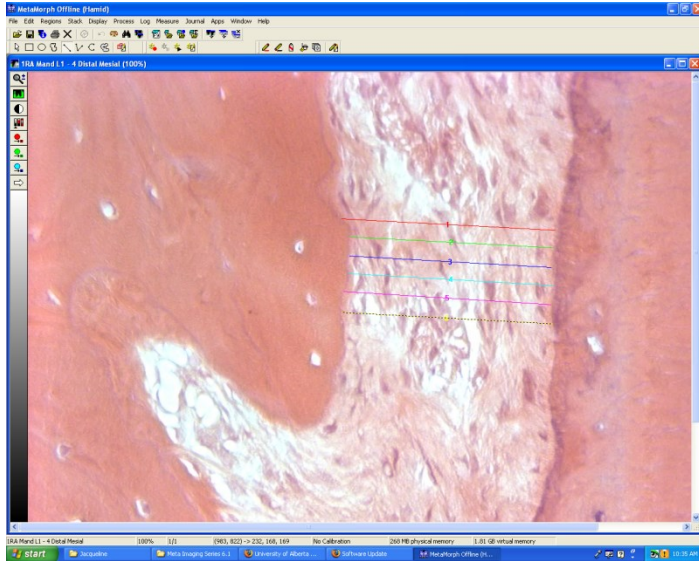


Figure 3-16: Histomorphometric analysis of PDL thickness (coloured lines).

PDL cell counting was completed by opening a new created image containing PDL tissue. “Measure” was selected followed by “Manually Count Object”. Each click on a cell was recorded by placing a “1” on the cells. To maintain a consistent area in which cell counts were performed, a line using the line tool was drawn along the length of the PDL. This line measured 30 $\mu$ m in every image. Two additional lines were drawn perpendicularly from both ends of the first line drawn. These perpendicular lines were extended beyond the thickness (width) of the PDL. Cells were counted only within the set area, which varied depending on the thickness of PDL (Figure 3-17). However, the length of PDL for the selected area always remained 30 $\mu$ m. To count PDL cells, a “1” was placed on each nucleus. “Manually Count Object” was re-opened and the number of cells was indicated by the count given in “Class 1”. This number was manually inserted into an excel spreadsheet for each measurement thereafter.

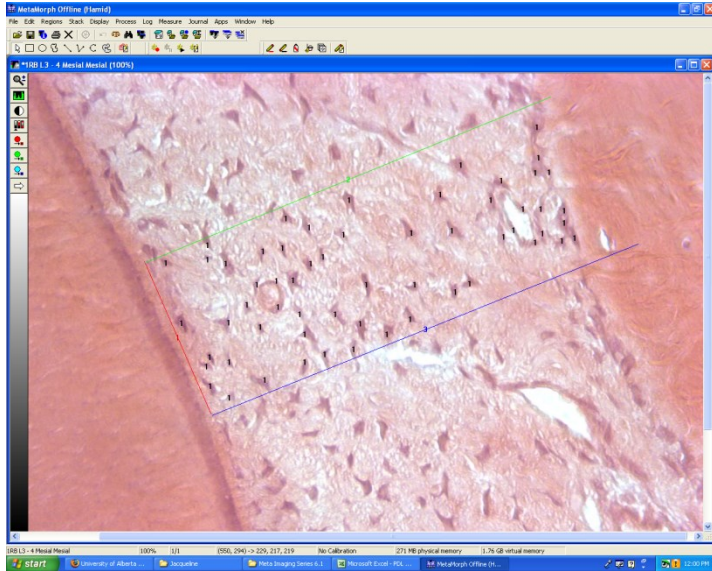


Figure 3-17: Histomorphometric analysis of PDL cell count.

Throughout these analyses using  $\mu$ CT and histomorphometry, the assessor was blinded to the treatment groups. After data collection was completed, all data was organized into treatment groups according to a labeling key. For the histomorphometric analyses, the data was further organized into compression and tensions sides at each of the three root levels.

### III.X. Statistical analysis

The mean of each treatment group was calculated along with their standard error of the mean. For these calculations, histomorphometric analyses only included the measurements for the mandible due to inconsistency and missing slides for samples from the maxillae. ANOVA with Tukey post hoc tests were used to compare the differences of the treatment groups to the negative control group in order to determine if there was a significant difference between each of

the treatments and the control group. For histomorphometric analysis, compression sides at each root level were compared to each other at the same root level, and tension sides at each root level were compared to each other also at the same root level. To determine statistically significant differences, a p-value of  $< 0.05$  was used.

## **Chapter IV: Results**

#### IV.I. Flowcytometry and ALP assay

Prior to assessing the effect of LIPUS and OIGFs on repair of OIRR in Beagle dogs, characterization of the gingival cells using MSC markers (Figure 4-1) and analysis of ALP activity of cultured GFs with and without LIPUS treatment (Figure 4-2) were performed.

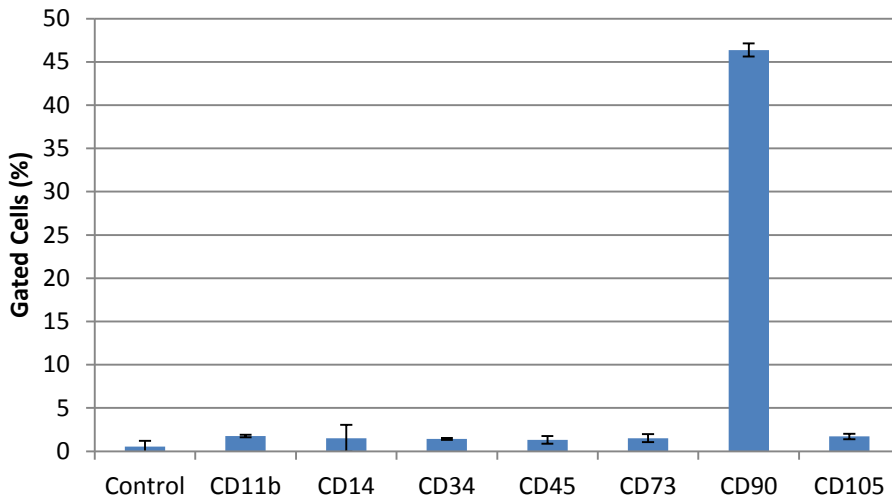


Figure 4-1: Immunophenotyping of canine gingival cells using flowcytometry with antibodies (CD11b, CD14, CD34, CD45, CD74, CD90, and CD105) to identify percentage of gated cells (%). FITC-conjugated Isotype-mouse IgG<sub>1</sub> and PE-conjugated Isotype-mouse IgG<sub>1</sub> were control antibodies.

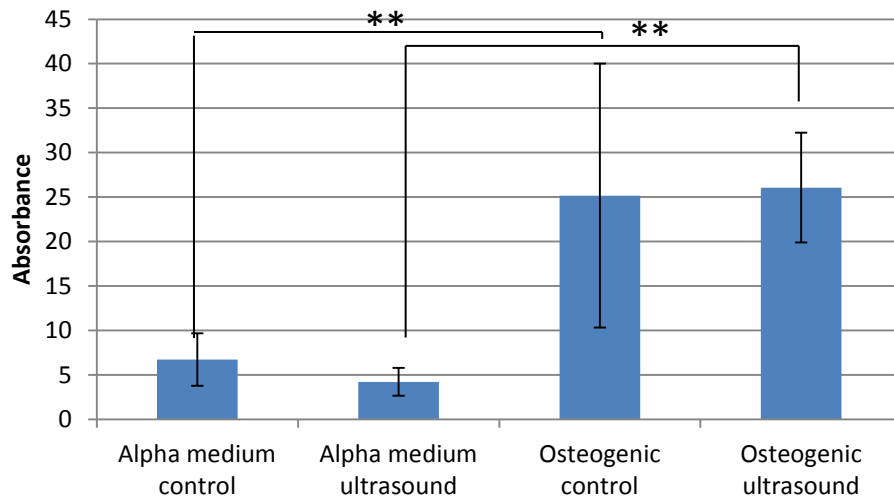


Figure 4-2: ALP assay showing ALP activity (absorbance level at 405nm) of canine gingival cells after four treatments – culture in medium without ultrasound, culture in medium with ultrasound, culture in osteogenic medium without ultrasound, and culture in osteogenic medium with ultrasound. (\*\* =  $p < 0.01$ )

#### IV.II. Histology and histomorphometric analysis

Histomorphometric analysis and micro-computed tomography analysis were performed in order to measure the effect of LIPUS and OIGFs on orthodontically induced root resorption in Beagle dogs. Digital histologic images were produced in order to measure the thickness of cementum, the width of the PDL, and to count PDL cells (Figure 4-3). The photos were taken on both the compression side and the tension side of the root in accordance with the direction of tooth movement during orthodontic treatment. Images were also produced at the coronal (level 1), middle (level 2), and apical (level 3) root levels since cementum and PDL thicknesses vary depending on the root level.

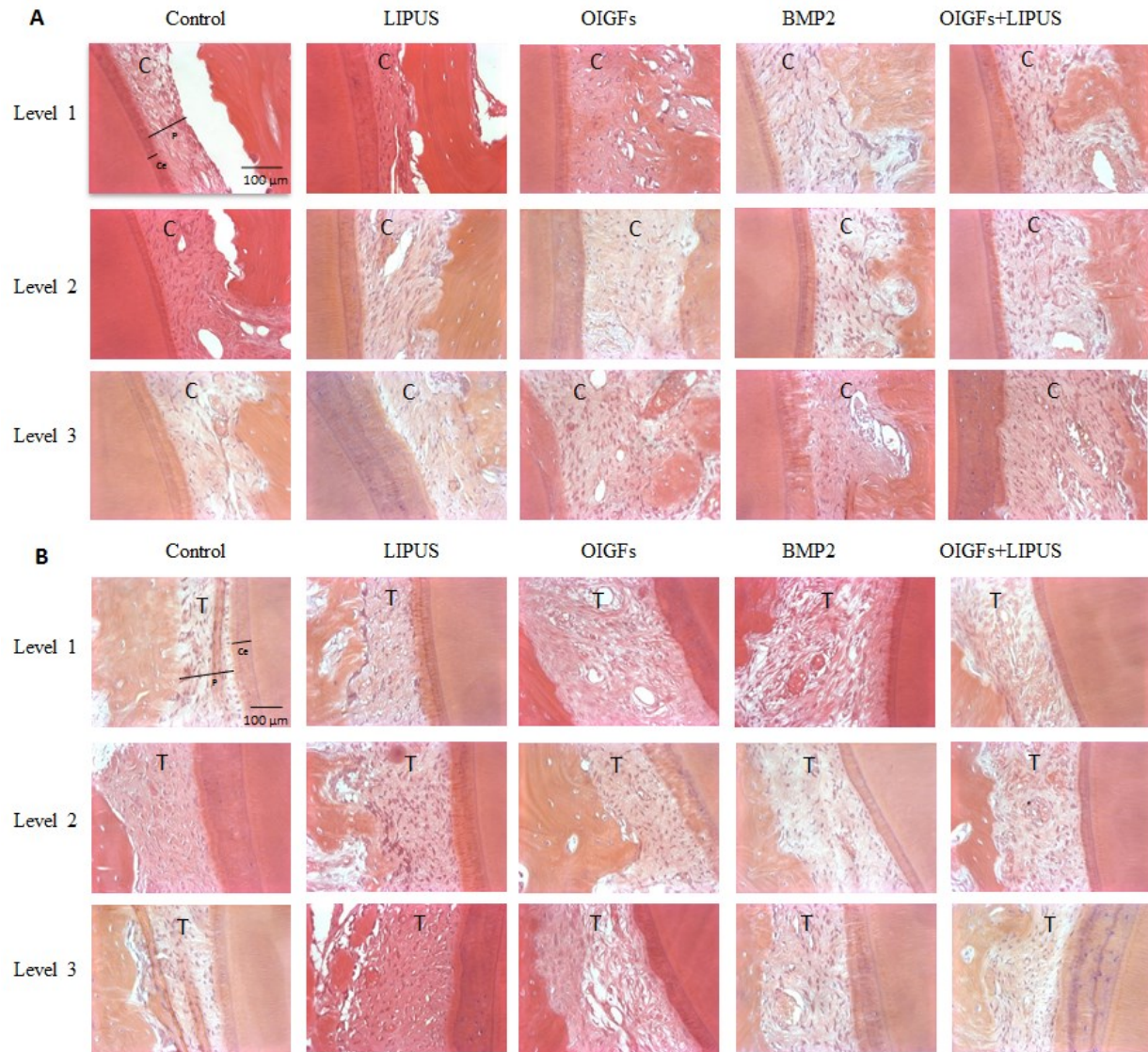


Figure 4-3: Digital histologic images of cementum and periodontal ligament from each treatment group on the compression (A) and tension (B) sides of the tooth root at coronal (level 1), middle (level 2), and apical (level 3) root levels. Cementum and periodontal ligament widths appear greater at the apical root level and in treatment groups compared to control. Scale bar = 100  $\mu$ m. P = PDL, Ce = Cementum. C = Compression side. T = Tension side.

Using the computer software MetaMorph Offline (Molecular Devices LLC, California), cementum thickness, PDL width, and PDL cell count were each measured for every tooth root in the mandible (Table 4-1). Statistical analyses were only performed to compare each treatment group to the control group in order to detect statistically significant differences. Significant differences were considered at  $p < 0.05$ .

Table 4-1: Cementum thickness ( $\mu\text{m}$ ) (mean  $\pm$  SEM), PDL width ( $\mu\text{m}$ ) (mean  $\pm$  SEM), and PDL cell count ( $\mu\text{m}$ ) (mean  $\pm$  SEM) in each treatment group on the compression (A) and tension (B) sides of the tooth root at coronal (level 1), middle (level 2), and apical (level 3) root levels.

\*Statistical comparison of treatment groups to control group only.

Treatment	Root Side and Level	Cementum Thickness ( $\mu\text{m}$ ) (mean $\pm$ SEM)	p-value*	PDL Width ( $\mu\text{m}$ ) (mean $\pm$ SEM)	p-value*	PDL Cell Count (mean $\pm$ SEM)	p-value*
Control	Compression Side						
	Level 1	22.74 $\pm$ 1.58	N/A	122.35 $\pm$ 15.24	N/A	51.09 $\pm$ 4.04	N/A
	Level 2	24.38 $\pm$ 5.02	N/A	142.54 $\pm$ 14.02	N/A	51.36 $\pm$ 3.74	N/A
	Level 3	28.11 $\pm$ 3.54	N/A	146.89 $\pm$ 14.65	N/A	63.78 $\pm$ 5.5	N/A
	Tension Side						
	Level 1	38.54 $\pm$ 4.36	N/A	106.07 $\pm$ 7.60	N/A	55.67 $\pm$ 4.15	N/A
	Level 2	43.07 $\pm$ 6.74	N/A	129.95 $\pm$ 8.52	N/A	4.92 $\pm$ 1.95	N/A
	Level 3	44.45 $\pm$ 6.21	N/A	139.20 $\pm$ 6.46	N/A	65.08 $\pm$ 5.76	N/A
	LIPUS	Compression Side					
Level 1		23.09 $\pm$ 2.82	1.000	119.77 $\pm$ 6.15	1.000	53.80 $\pm$ 3.79	0.994
Level 2		25.53 $\pm$ 3.37	1.000	134.25 $\pm$ 7.79	0.991	54.10 $\pm$ 3.71	0.987
Level 3		53.63 $\pm$ 8.35	0.049	141.07 $\pm$ 13.78	0.998	54.50 $\pm$ 4.40	0.578
Tension Side							
Level 1		36.93 $\pm$ 3.62	0.999	132.88 $\pm$ 13.33	0.265	60.10 $\pm$ 5.40	0.947
Level 2		33.41 $\pm$ 2.00	0.599	128.34 $\pm$ 10.80	1.000	74.30 $\pm$ 7.41	0.0002
Level 3		67.34 $\pm$ 6.85	0.281	173.77 $\pm$ 17.60	0.529	76.67 $\pm$ 7.18	0.805
OIGFs		Compression Side					
	Level 1	28.78 $\pm$ 4.18	0.597	152.72 $\pm$ 14.88	0.396	61.80 $\pm$ 6.01	0.506
	Level 2	29.85 $\pm$ 3.98	0.781	124.04 $\pm$ 11.24	0.834	52.09 $\pm$ 4.67	1.000
	Level 3	31.72 $\pm$ 6.27	0.995	155.30 $\pm$ 18.36	0.993	60.29 $\pm$ 4.66	0.983
	Tension Side						
	Level 1	40.51 $\pm$ 3.22	0.997	133.51 $\pm$ 9.37	0.165	55.88 $\pm$ 3.73	1.000
	Level 2	39.34 $\pm$ 4.31	0.971	154.63 $\pm$ 11.42	0.329	64.20 $\pm$ 3.47	0.033
	Level 3	34.44 $\pm$ 5.36	1.000	152.17 $\pm$ 18.13	0.973	60.67 $\pm$ 5.12	1.000
	BMP2	Compression Side					
Level 1		20.48 $\pm$ 1.34	0.985	152.84 $\pm$ 6.53	0.496	58.50 $\pm$ 4.53	0.803
Level 2		18.35 $\pm$ 1.39	0.801	137.75 $\pm$ 9.74	0.999	56.30 $\pm$ 3.83	0.898
Level 3		42.22 $\pm$ 375	0.464	151.08 $\pm$ 11.35	1.000	56.11 $\pm$ 4.41	0.714
Tension Side							
Level 1		36.50 $\pm$ 4.98	0.997	112.67 $\pm$ 7.68	9.988	64.00 $\pm$ 4.47	0.668
Level 2		28.91 $\pm$ 2.77	0.179	148.95 $\pm$ 12.69	0.695	58.22 $\pm$ 3.91	0.287
Level 3		58.84 $\pm$ 4.72	0.702	152.36 $\pm$ 13.94	0.971	55.88 $\pm$ 2.98	0.946
OIGFs +LIPUS		Compression Side					
	Level 1	22.49 $\pm$ 3.34	1.000	124.50 $\pm$ 11.69	1.000	57.80 $\pm$ 5.40	0.853
	Level 2	19.89 $\pm$ 1.34	0.898	161.28 $\pm$ 16.49	0.814	64.44 $\pm$ 3.48	0.164
	Level 3	57.07 $\pm$ 6.85	0.015	127.93 $\pm$ 11.48	0.877	56.88 $\pm$ 2.73	0.803
	Tension Side						
	Level 1	44.68 $\pm$ 5.79	0.855	1.2533 $\pm$ 2.31	0.589	60.92 $\pm$ 4.49	0.891
	Level 2	26.34 $\pm$ 12.32	0.089	1.4353 $\pm$ 6.37	0.842	67.92 $\pm$ 4.87	0.002
	Level 3	76.37 $\pm$ 11.01	0.052	160.48 $\pm$ 14.40	0.819	81.73 $\pm$ 9.06	0.043

Cementum thickness was measured on both sides of the root (compression and tension) and at three root levels (Figure 4-4). Statistical analyses using ANOVA with Tukey post hoc tests to compare the treatment groups to the control group reveal that on the compression side of the root and at the apical root level the LIPUS group and the OIGFs+LIPUS group had significantly greater cementum thickness than the control group ( $p < 0.05$ ). Although similar results were found on the tension side of the root, no statistical significance was calculated.

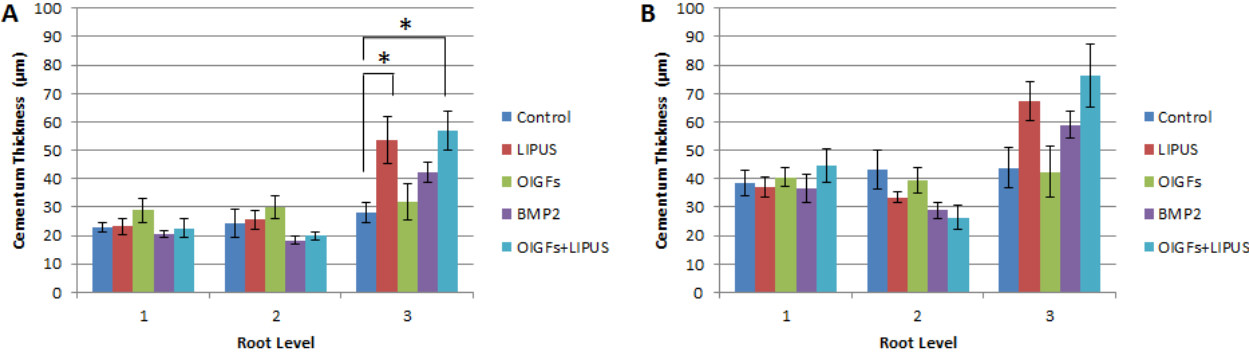


Figure 4-4: Cementum thickness ( $\mu\text{m}$ ) (mean  $\pm$  SEM) in each treatment group on the compression (A) and tension (B) sides of the tooth root at coronal (level 1), middle (level 2), and apical (level 3) root levels. (\* =  $p < 0.05$ ).

Using similar methods, the PDL width was measured on both the tension and compression sides of the root and also at three root levels (Figure 4-5). No statistically significant differences were found between each of the treatment groups compared to the control group.

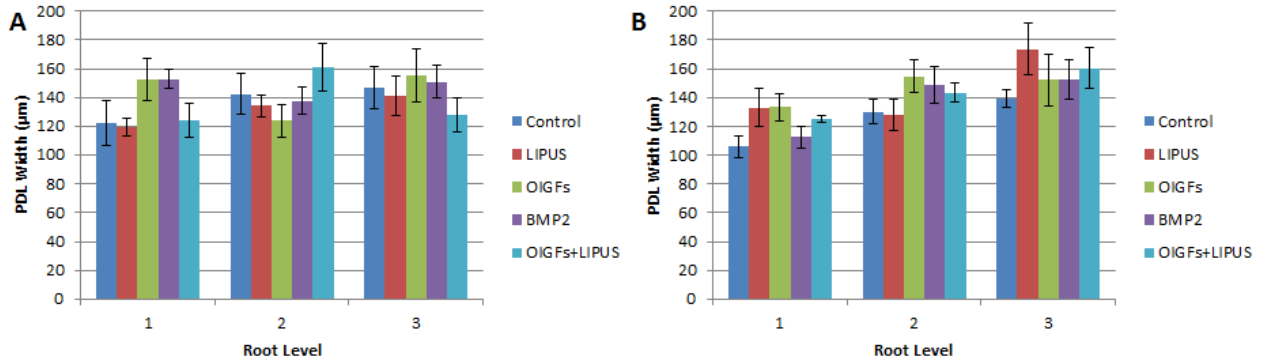


Figure 4-5: Periodontal ligament width ( $\mu\text{m}$ ) (mean  $\pm$  SEM) in each treatment group on the compression (A) and tension (B) sides of the tooth root at coronal (level 1), middle (level 2), and apical (level 3) root levels.

Next, cells in the PDL were counted according to the methods in Chapter III. Using ANOVA with Tukey post hoc tests, it was revealed that there were statistically significant differences between the control group and the treatments groups only on the tension side of the root (Figure 4-6). At the middle root level the LIPUS group, the OIGFs group, and the OIGFs+LIPUS group each had a significantly greater number of PDL cells compared to the control group ( $p < 0.01$ ,  $p < 0.05$ , and  $p < 0.01$ , respectively). Also, at the apical root level, the OIGFs+LIPUS group had a significantly greater number of PDL cells compared to the control group at the same level.

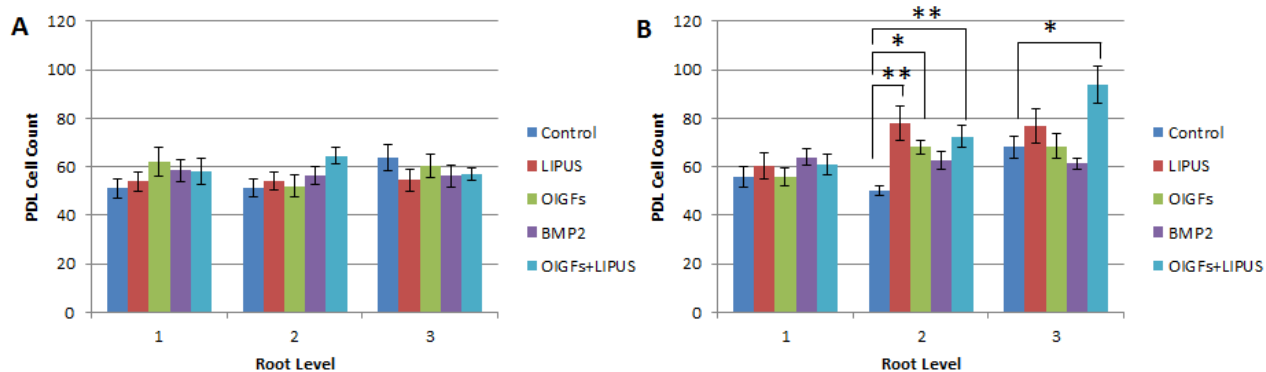


Figure 4-6: Periodontal ligament cell count (mean  $\pm$  SEM) in each treatment group on the compression (A) and tension (B) sides of the tooth root at coronal (level 1), middle (level 2), and apical (level 3) root levels. (\* =  $p < 0.05$ , \*\* =  $p < 0.01$ ).

#### IV.III. $\mu$ CT analysis

The tooth roots from the maxilla and mandible of each Beagle dog were analyzed using micro-computed tomography in order to measure root lengths, root resorption lacunae depths, root resorption lacunae lengths, and root resorption lacunae volumes in each of the treatment groups (Figure 4-7; Table 4-2). Statistical analysis using ANOVA with Tukey post hoc tests was used to only compare each of the treatment groups to the control group.

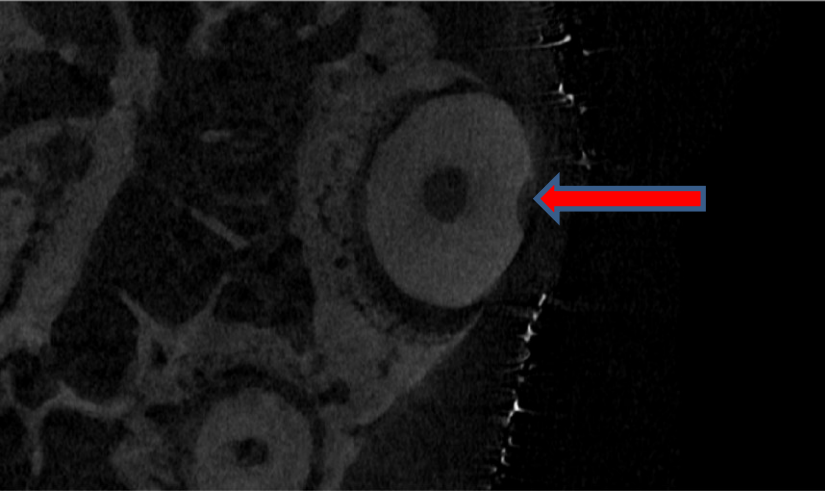


Figure 4-7:  $\mu$ CT reconstructed image of a tooth root with evidence of orthodontically induced root resorption (red arrow).

Table 4-2: Root lengths (mm) (mean  $\pm$  SEM), root resorption lacunae depth (mm) (mean  $\pm$  SEM), root resorption lacunae length (mm) (mean  $\pm$  SEM), and root resorption lacunae volume (mm<sup>3</sup>) (mean  $\pm$  SEM) in each treatment group.

<b>Treatment</b>	<b>Root Length (mm) (mean <math>\pm</math> SEM)</b>	<b>p-value*</b>	<b>Resorption Lacunae Depth (mm) (mean <math>\pm</math> SEM)</b>	<b>p-value*</b>	<b>Resorption Lacunae Length (mm) (mean <math>\pm</math> SEM)</b>	<b>p-value*</b>	<b>Resorption Lacunae Volume (mm<sup>3</sup>) (mean <math>\pm</math> SEM)</b>	<b>p-value*</b>
<b>Control</b>	9.6651 $\pm$ 0.3409	N/A	0.1204 $\pm$ 0.0182	N/A	0.8445 $\pm$ 0.0663	N/A	0.0688 $\pm$ 0.0146	N/A
<b>LIPUS</b>	10.6217 $\pm$ 0.5201	0.520	0.0808 $\pm$ 0.0060	0.010	0.7939 $\pm$ 0.0587	0.981	0.0237 $\pm$ 0.0038	0.000035
<b>OIGFs</b>	10.1884 $\pm$ 0.4478	0.897	0.0831 $\pm$ 0.0054	0.037	0.7918 $\pm$ 0.0798	0.982	0.0378 $\pm$ 0.0072	0.018304
<b>BMP2</b>	10.3670 $\pm$ 0.5588	0.807	0.0790 $\pm$ 0.0064	0.018	0.7653 $\pm$ 0.0569	0.937	0.0312 $\pm$ 0.0036	0.000921
<b>OIGFs +LIPUS</b>	9.3827 $\pm$ 0.3300	0.989	0.0718 $\pm$ 0.0054	0.002	0.7758 $\pm$ 0.0606	0.957	0.0281 $\pm$ 0.0030	0.000179

\*Statistical comparison of treatment groups to control group only.

$\mu$ CT analysis of root lengths reveals that although the LIPUS group, the OIGFs group, and the BMP2 group had the longest roots, there were no statistically significant differences between each of the treatment groups compared to the control group (Figure 4-8).

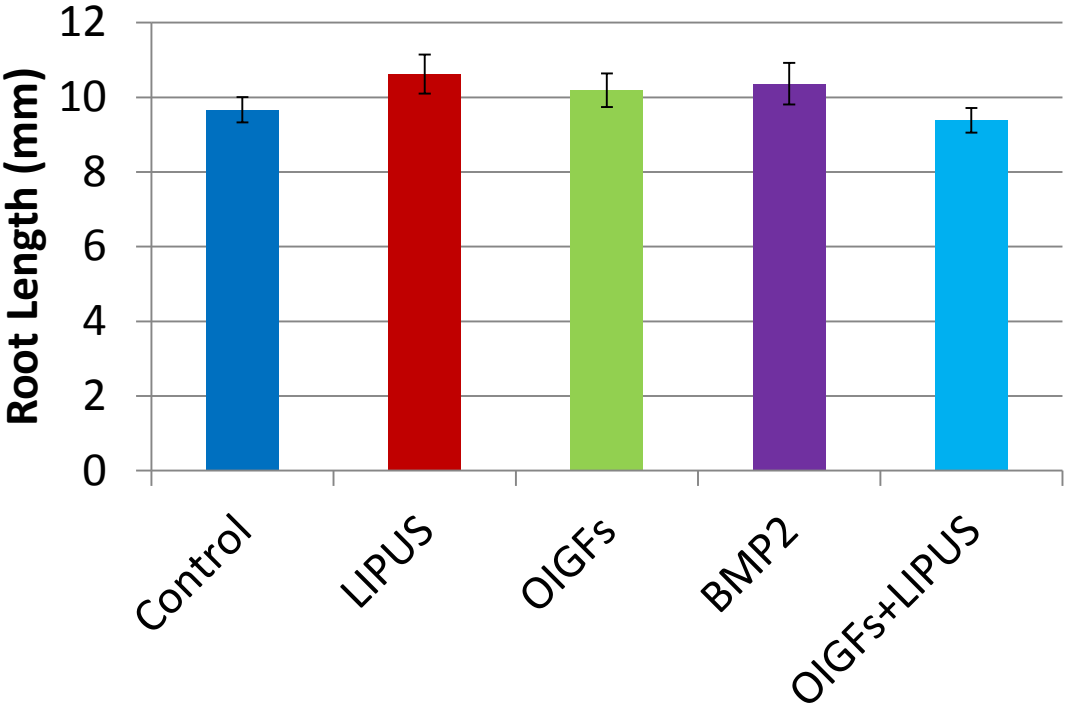


Figure 4-8: Root length (mm) (mean  $\pm$  SEM) as evaluated by  $\mu$ CT analysis in each treatment group.

Further analyses revealed that the control group had the deepest root resorption lacunae ( $0.1204 \pm 0.0182$  mm) (Figure 4-9). This group had statistically significantly deeper lacunae compared to each of the treatment groups – LIPUS ( $p < 0.05$ ), OIGFs ( $p < 0.05$ ), BMP2 ( $p < 0.05$ ), and OIGFs+LIPUS ( $p < 0.01$ ).

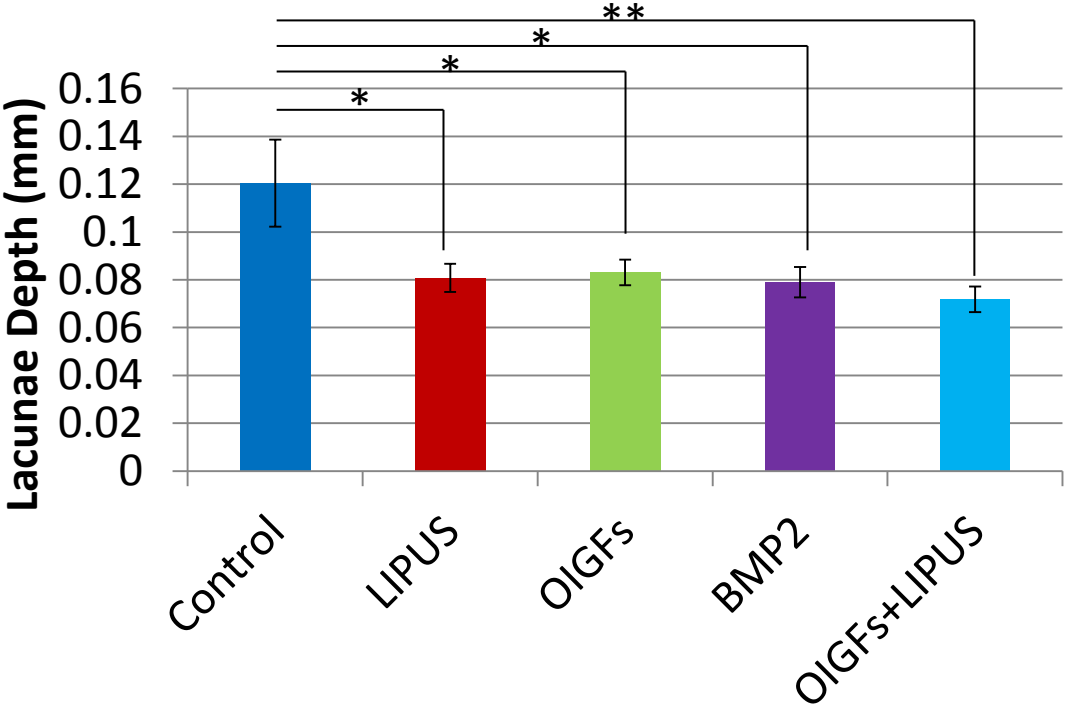


Figure 4-9:  $\mu$ CT analysis of root resorption lacunae depth (mm) (mean  $\pm$  SEM) in each treatment group. (\* =  $p < 0.05$ , \*\* =  $p < 0.01$ ).

Measurements of lacunae length show that the control group had longer resorption lacunae compared to the treatment groups, however, using ANOVA with Tukey post hoc tests, no statistically significant differences were found between the control group lacunae lengths compared to each of the treatment groups' lacunae lengths (Figure 4-10).

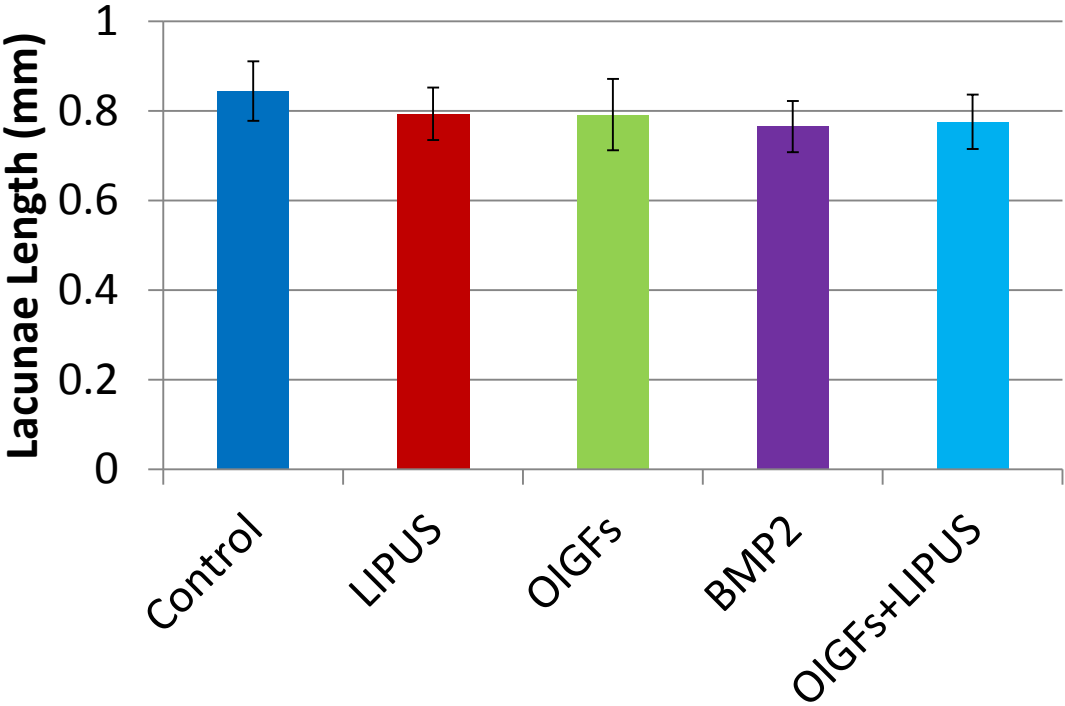


Figure 4-10:  $\mu$ CT analysis of root resorption lacunae length (mm) (mean  $\pm$  SEM) in each treatment group.

Finally, the volume of each resorption lacunae was measured (Figure 4-11). The control group showed the greatest volume of lacunae ( $0.0688 \pm 0.0146 \text{ mm}^3$ ), and statistical analyses using ANOVA with Tukey post hoc reveal that these volumes were statistically significantly greater than each of the treatment groups' volumes – the LIPUS group ( $p < 0.0001$ ), the OIGFs group ( $p < 0.05$ ), the BMP2 group ( $p < 0.001$ ), and the OIGFs+LIPUS group ( $p < 0.001$ ).

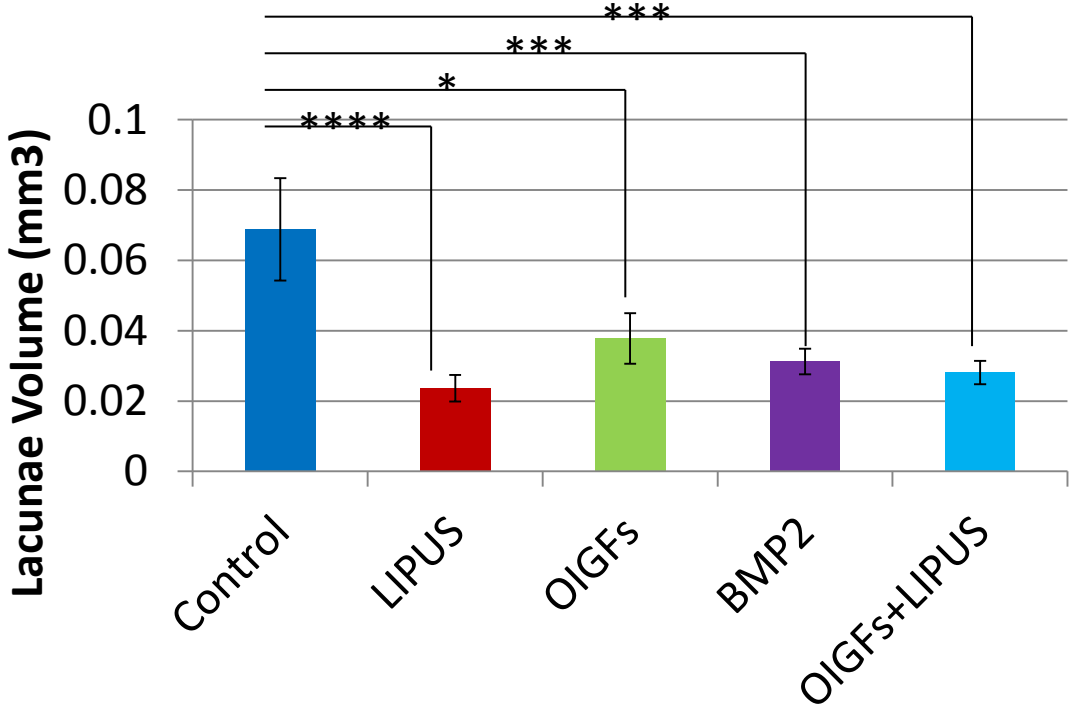


Figure 4-11:  $\mu$ CT analysis of root resorption lacunae volume ( $\text{mm}^3$ ) (mean  $\pm$  SEM) in each treatment group. (\* =  $p < 0.05$ , \*\*\* =  $p < 0.001$ , \*\*\*\* =  $p < 0.0001$ ).

## **Chapter V: Discussion**

This research study evaluated the effect of low intensity pulsed ultrasound and osteogenically induced gingival fibroblasts on repair of orthodontically induced root resorption in Beagle dogs. To measure the repair effects of these two methods, local injection of OIGFs and application of LIPUS, on OIRR, cementum thickness, PDL width, and PDL cell count were evaluated through histology and histomorphometric analysis, and root length and root resorption lacunae length, depth, and volume were measured using micro-computed tomography.

#### **V.I. Osteogenically induced gingival fibroblasts**

Characterization of mesenchymal stem cells is an important step in their potential use in periodontal repair, specifically in repair of orthodontically induced root resorption. A preliminary study using gingival cells obtained from the dogs in this study used flowcytometry to identify cell surface markers found on mesenchymal stem cells in order to properly characterize them (Figure 4-1). This classification of canine gingival cells is also necessary for translational research into clinical experiments from preclinical animal studies, such as the present study using Beagle dogs. In this preliminary study, canine gingival cells were treated with LIPUS for a total of 20 minutes for one day. The antibodies used to detect corresponding cell surface markers were CD11b, CD14, CD34, CD45, CD73, CD90, and CD105. Dominici et al. (2006) address the issue of many ambiguities and inconsistencies being created in the field of mesenchymal stromal/stem cell research. The International Society for Cellular Therapy (ISCT) report that multipotent mesenchymal stromal cells is the term that is currently used for plastic-adherent cells that have been isolated from bone marrow and other tissues, and that

these cells are often also called mesenchymal stem cells (Horwitz et al., 2005). The defining characteristics of MSCs appear to be inconsistent among investigators because many laboratories have developed a variety of methods and techniques to isolate and expand MSCs. The Mesenchymal and Tissue Stem Cell Committee of the ISCT has proposed a set of standards to define human MSCs to be used in both laboratory-based investigations and pre-clinical studies. Three criteria have been proposed:

1. Adherence to plastic
2. Specific surface antigen expression
3. Multipotent differentiation potential

The concurrent study to identify stem cell characteristics of the canine gingival cells did not employ plastic adherence as one of the criteria for defining MSCs. However, the study did attempt to identify most of the proposed surface antigens. These proposed antigens are CD105, CD73, CD90, CD45, CD34, CD14 (or CD11b), CD19 (or CD 79 $\alpha$ ), and human leukocyte antigen-DR (HLA-DR). Positive expression ( $\geq 95\%$ ) of CD105, CD73, and CD90 must be present, and there must be negative expression ( $\leq 5\%$ ) of CD45, CD34, CD14 (or CD11b), CD19 (or CD79 $\alpha$ ), and HLA-DR. The concurrent study did not include identification of CD19 (or CD79 $\alpha$ ) nor the identification of HLA-DR. Expression of each of these markers was under 5%, with the exception of CD90, which expressed at about 45%. To identify cells as mesenchymal stem cells, these cells must express CD73, CD90, and CD105 more than 95%. Based solely on the lack of expression of CD73 and CD105 by these cells, these results lead to the suggestion that these cells cannot be identified as true stem cells, and can only be referred to as fibroblasts. Although the expression of CD90 was greater than the expression of CD73

and CD105, this expression was still much less than 95%. This also supports the suggestion that these canine gingival fibroblast cells may not be considered as stem cells. These results may also suggest that the population of cells obtained were not a homogeneous cell population, therefore leading to the decreased expression of CD90, CD73, and CD105. The types of cells that may have been present in the injection include mesenchymal stem cells, epithelial cells, phagocytic cells, but possibly other types as well. Based solely on the methods of this concurrent study, other cell types that may have been included were not able to be identified.

Further preliminary studies demonstrated the differentiation potential of similar human gingival cells. The cells were successfully differentiated into an osteogenic phenotype (Wong et al., 2008), into a cementoblast phenotype (Mostafa et al. 2008b), and into neural-like cells (El-Bialy et al., 2014). According to the proposed criteria for defining MSCs, these cells have the ability to be differentiated *in vitro* into osteoblasts, adipocytes, and chondroblasts (Dominici et al., 2006). A preliminary study differentiated gingival cells into osteogenic cells (Wong et al., 2008). There is currently no study that has differentiated canine gingival cells into adipogenic nor chondroblastic cells. Although flowcytometry suggests that the population of cells may not be entirely mesenchymal stem cells, the differentiation potential of these cells may show that mesenchymal stem cells were present in this population. Additional studies are required in order to fully identify canine gingival cells as potential mesenchymal stem cells.

After the gingival cells were isolated in the previous study, the cells were subject to culture in osteogenic medium and LIPUS application and the levels of ALP activity were measured (Figure 4-2). Gingival cells were cultured in four treatment groups. The first group was cultured in an alpha medium and did not receive further treatment. The second group was

cultured in the same medium but also received LIPUS treatment for 20 min/day for four weeks. The third group was cultured in an osteogenic medium and received no further treatment. Finally, the fourth group was cultured in the osteogenic medium and also received LIPUS treatment in the same manner as the second group. ALP activity, which was indicated by absorbance level, was significantly greater in the osteogenic control group compared to the alpha medium control group ( $p < 0.01$ ), and ALP activity was significantly greater in the osteogenic ultrasound group compared to the alpha medium ultrasound group ( $p < 0.01$ ). The results showed that the canine gingival cells expressed higher ALP when cultured in osteogenic medium but also when cultured in this medium and with LIPUS treatment. It is also interesting to mention that although the difference between the osteogenic control group and osteogenic LIPUS group was statistically non-significant, LIPUS did increase ALP activity. This suggests that LIPUS may have a greater effect on inducing osteogenic differentiation in combination with osteogenic medium than when only osteogenic medium is employed. Since the gingival cells in the present study were also cultured in osteogenic medium and received LIPUS treatment for 20 minutes per day for four weeks, these cells can be considered as osteogenic induced gingival fibroblasts.

## **V.II. Histomorphometric analysis**

Observation of the histological digital photos reveals that cementum and PDL appeared to be generally thicker around the apex (Level 3) of tooth root compared to the middle (Level 2) or coronal (Level 1) levels (Figure 4-3). This is in agreement with previous literature that showed

that cementum increases in thickness towards the apex and PDL is widest at the coronal and apical levels of the tooth root (Bosshardt and Selvig, 1997; Nanci and Bosshardt, 2006).

To quantitatively determine the effect of LIPUS and OIGFs on repairing OITRR caused by orthodontic bodily tooth movement for four weeks, first, the periodontal tissues were measured using histomorphometric analysis. Cementum thickness measurements were performed on both the compression and tension sides of the tooth root because the effects of orthodontic tooth movement on these tissues vary depending on the side of the root (Figure 4-4). These measurements were also completed at three root levels because the thickness of the tissues also varies depending on the level's distance from the root apex. On the compression side of the root, there were no significant differences in cementum thickness between each of the treatment groups and control group at the coronal and middle levels. However, at the apical third of the root, the LIPUS group and the OIGFs+LIPUS group both had significantly greater cementum thickness compared to the control group ( $p < 0.05$ ). Although the combination treatment group (OIGFs+LIPUS) was only slightly greater than the group that only received LIPUS treatment, it may be possible that LIPUS had a synergetic effect on OIGFs, which lead to increased cementogenesis. It also seems that compression forces, which are increased at the apical area of the tooth root, may have antagonized the stimulatory effect of OIGFs on cementum formation that was hypothesized in this study. This was shown by the non-significant difference between the OIGFs group and the control group at the apical root level. It appears that it may be possible that this decreased effect of OIGFs on cementum formation may be balanced by the stimulatory effect of LIPUS on these cells at the apical third of the root, since the combination treatment group had greater cementum thickness compared to the group that only received LIPUS treatment, as previously stated. It is also important to note that

the location of the OIGFs injection may have an effect on cementum thickness when compared between the groups. Since OIGFs were injected near the apex, there may have been a greater number of these cells at the apex to be stimulated by LIPUS, and therefore at the coronal and middle levels, LIPUS would not have had as great of an effect on these cells due to their potential absence.

The present study evaluated the viability of the cells post-injection with a 30-gauge needle before the actual cell injection was performed. Another study reported that the diameter of 20-, 25-, and 30-gauge needles had no effect on MSC viability after injection (Walker et al., 2010). This study further characterized the cells post-injection and compared these cells' surface markers to those of cells that did not pass through a needle. No difference in characterization was found. If the current study had employed one type of cell in the injection and characterization using cell surface markers was determined for this one type of cell, then it would have been appropriate to perform the same comparison between cells post-injection and cells that were not injected through a needle.

A previous study that evaluated the effect of LIPUS on cementum thickness in beagle dogs undergoing orthodontic tooth movement demonstrated similar results to the current study (Al-Daghreer et al., 2014). In this study cementum thickness was significantly greater in the LIPUS-treated group compared to the control group at the apical third of the tooth root.

Similar results were observed and measured on the tension side of the root, however, no statistically significant difference were found between the LIPUS group and OIGFs group compared to the control group although these two groups showed greater cementum thickness also at the apical third of the root. Also on this side, the OIGFs group showed increased effect

of cementum thickness at the coronal level only, although this was statistically non-significant. It may be possible that these injected cells may have moved coronally, causing their effect to be more obvious at this level compared to the apical level.

Since it is unknown as to the exact location of the OIGFs post-injection, this warrants future studies involving natural long term labeling. This cell labeling would allow for tracking of these cells after injection, and for assertive evidence that these cells were successfully incorporated into the periodontal tissues of cementum and PDL and also to determine their migration if present. Currently, there is no long-term labeling for such cells available which is appropriate for this type and length of study.

The decreased effect of OIGFs on the tension side of the root may be explained by the possibility of a tipping movement being present in this study, even though the intention was solely to produce bodily movement using thicker wire in orthodontic tubes. Since no counter moments were added to the force system, it may be possible that what is labeled as the tension side of the root at the coronal level, may actually be the compression side. The tension forces seemed to have produced increased cementum thickness compared to compression forces, which may explain the cementum thickness decrease in the OIGFs group on the tension side from the coronal to middle levels compared to the compression side of the root.

It is interesting to note that there were statistically significant differences on the compression side of the tooth root and none on the tension side of the root. The compression side of the root would generally have greater damage caused by OIRR due to clastic cellular activity that would be evident by thinner cementum. It may be possible that the repair effect of LIPUS and OIGFs is even greater when this difference in pressure exerted on the root is considered.

It also worth noting that the BMP-2 injection led to greater cementum thickness compared to the control group. In a previous study, application of BMP-2 to tooth root defects resulted in cementum-like tissue formation compared to control root defects that did not receive BMP-2 treatment (Miyaji et al., 2010). This study's results are comparable to the present study's results of increased cementum thickness. Even though this difference was statistically non-significant and cementum thickness was less than either of the LIPUS and OIGFs+LIPUS groups, it may also have potential in repair of OIRR in dogs or even in humans.

Similar to the cementum thickness evaluations, PDL width was measured in each group on the compression and tension sides of the root at coronal, middle, and apical root levels (Figure 4-5). The OIGFs group had greater PDL thickness at coronal and apical levels compared to control on the compression side, and the OIGFs+LIPUS group also had greater PDL width compared to the control group but at the middle level. However, there were statistically non-significant differences found between these groups compared to the control group. This increased PDL width may be due to the reparative effect of OIGFs on cementum and also on the possible antagonizing effect of these cells on osteoclast activity (de Vries et al., 2006), which would otherwise have increased alveolar bone resorption and decreased PDL thickness.

On the tension side of the root, PDL thickness in the LIPUS group at the coronal and apical levels, in the OIGFs group at each root level, and in the OIGFs+LIPUS group at each root level was greater than the control at the corresponding root level. Although these differences were not statistically significantly different, similar results were found concerning PDL width in LIPUS-treated groups compared to control groups in a previous study (Al-Daghreer et al., 2014). In this study, it was demonstrated that although PDL thickness was greater on various

sides of the tooth root and at each root level, the differences between LIPUS-treated roots and control roots were not significantly different.

Finally, PDL cell counts were performed in each group on compression and tension sides at each root level (Figure 4-6). These measurements show that the LIPUS group, the OIGFs group, and the OIGFs+LIPUS group each had a greater number of PDL cells compared to the control group at each root level on the tension side of the root. The cell counts in these groups were statistically significantly different from the control group at the middle root level ( $p < 0.01$ ,  $p < 0.05$ , and  $p < 0.01$ , respectively), however, only the OIGFs+LIPUS group had a significantly greater number of PDL cells compared to the control group at the apical root level ( $p < 0.05$ ). Although similar results were found at the coronal and middle root levels on the compression side, PDL cellularity of these groups compared to the control group was not significantly different. Al-Daghreer et al. (2014) also demonstrated insignificant differences in PDL cellularity when comparing between LIPUS-treated groups and control groups at middle and apical levels.

Although PDL cell counts were performed, an actual measurement of proliferation of these cells was not performed. Ki-67 is a protein that is strictly associated with cell proliferation (Scholzen and Gerdes, 2000). Ki-67 is present during all active phases of the cell cycle (G1, S, G2, and mitosis) and is absent in resting cells (G0). Use of this marker in the present study would have aided in determining the presence of PDL proliferation as a result of LIPUS application and/or OIGF injection.

A correlation between PDL width and cellularity was expected in the current study, however, there was no significant difference in PDL width found between each of the treatment groups

and the control group, but there was a significant difference in cell count found between the groups. Since the thickness of PDL did not change, but the PDL cell count was significantly greater in the treatment groups compared to the control on the tension side of the root, PDL cell density must have increased in these corresponding groups compared to the control. A report on PDL fibroblast density age-related changes found that cell density decreased with age when comparing PDL cell density in younger patients to older patients (Krieger et al., 2013). This study suggested that this decreased cell density may cause a delay in PDL remodeling. It may be possible that this delay may cause decreased repair of the PDL after root resorption has occurred. Therefore, an increased PDL cell density, as measured in the present study, may be correlated with increased repair potential after OIRR has taken place. Another explanation of the non-correlation may be a possible equilibrium of PDL width. Although cell number may increase, PDL width may have the capacity to increase to a particular width. If this maximum thickness was achieved, then no further increase would have been measured. It is also to be noted that although an increase in PDL cellularity may indicate repair, it may also be related to inflammation, which may be followed by cell death.

A previous *in vitro* study that investigated the effects of LIPUS on human gingival fibroblasts found that LIPUS did not significantly increase proliferation in human GFs (Mostafa et al., 2009). This study, however, only exposed these cells to LIPUS for 5-minute and 10-minute periods per day, which is less than the current study, which used 20-minute periods per day. It may be possible that a longer exposure to LIPUS would cause an increase in cell proliferation, and that the effect of LIPUS on GFs would be increased in an *in vivo* study.

Although the present study combined mandibular and maxillary data, there may have been a difference in the effectiveness of the two treatment modalities between upper and lower premolars. Preliminary analysis of separate maxillary and mandibular data revealed that there was more significant difference between maxillary and mandibular premolars, however, this data is not shown.

This study's results suggest the presence of a reparative process as a direct result of LIPUS and/or OIGFs. However, it may be possible that the increased cementum that was measured in each group at varying degrees is due to a protective process as opposed to repair. The current study did not use a group of roots that was not manipulated by orthodontic tooth movement, since each premolar received bodily movement. If a non-manipulated control was employed, then a comparison between this group and the others may be able to determine whether or not repair or a protective process happened.

The present study only measured the thickness of cementum and did not examine the structural characteristics of such tissue. Measuring the thickness of new and old cementum would provide additional information to support or refute the effectiveness of the treatment modalities in repair of OIRR. This would be performed by examining cement lines, also referred to as reversal lines (Yamamoto et al., 2000). These lines are indicators of new cementum attachment.

It was hypothesized in the present study that after OIGFs injections and LIPUS treatment, cementum thickness, PDL width, and PDL cellularity would be significantly greater compared to the control group. LIPUS has been shown to enhance cellular differentiation of gingival cells into cementoblast-like cells and also to increase cellular proliferation (Inubushi et al.,

2008; Doan et al., 1999). Based on these results, it was expected that the combination of LIPUS and OIGFs would have resulted in greater cementum thickness, PDL width, and PDL cellularity compared to not only the control, but also compared to the LIPUS group and the OIGFs group where either treatment is applied alone and not in combination with one another. Also, the results from the ALP assay showed that the application of only LIPUS seemed to not have an effect on ALP activity and therefore mineralization by the gingival cells. However, *in vivo* there appeared to be an effect of LIPUS on cementum thickness. This contradiction may be explained by differing mechanisms between *in vitro* and *in vivo* in reference to cell growth and activity. However, a definitive explanation of this contradiction is unknown.

Since the type of tooth movement was not tested and only assumed based on the tooth movement system created, a combination a different tooth movements including tipping, torque and bodily may have caused the variety of expected and unexpected results. Further studies that monitor the type of tooth movement are required in order to support or clarify our results.

Also, the incorporation of OIGFs into the PDL tissues was not possible to be observed based on the limitation of long-term cell labeling. Future studies that employ this method may be able to explain the variety of results in the present study. Tracking these cells would also be important for translating this pre-clinical animal study into clinical studies. Determining the exact location of these injected cells would either rule out or support the speculation in the present study that these cells may have migrated from the apical area to the middle and coronal root levels and the possibility of this cellular movement varying between tooth roots depending

on the location of the premolar and on the pressure exerted by force application on the tooth root.

### **V.III. $\mu$ CT analysis**

Micro-computer tomography ( $\mu$ CT) analysis was performed in order to determine the extent of OIRR through observation and measurement of root resorption lacunae in each treatment group compared to the control group. Prior to the measurements, the lengths of the tooth roots were evaluated (Figure 4-8). There are three degrees of severity of OIRR, as described in section I.I (Brezniak and Wasserstein, 2002). The first degree is surface resorption, which only affects the outer layer of root cementum. The second degree is deep resorption. This degree of severity involves the resorption of cementum and outer layer of dentin. Finally, the third degree, circumferential apical root resorption, includes full resorption of hard tissue components at the apex of the tooth root. This degree is also known as severe root resorption and results in evidence of root shortening since dental tissues are fully resorbed around the circumference of the root apex. Analysis of root length reveals that the longest roots were in the groups that received LIPUS treatment, injection of OIGFs, and application of BMP-2. The results show that the control group and the OIGFs+LIPUS group had the shortest roots. Even though these root lengths varied slightly, there were no statistically significant differences between each of the treatment groups and the control group. It was expected that a greater degree of severe root resorption would be evident in the control group compared to each of the other treatment groups, which although was present, these root length measurements show that the combination treatment group (OIGFs+LIPUS) group had the shortest root lengths compared to

each of the other treatment groups and the control group. These results may have occurred based on the initial root lengths before the beginning of the study. Since initial root lengths were not determined, a comparison between root lengths before treatment and after treatment cannot be performed. It may be possible that the mean root length in the OIGFs+LIPUS group before treatment was significantly shorter compared to each of the other groups. If this was the case, then there may have been a significant increase in root length in this group, and this difference in root length may have resulted in a significantly greater increase in root length compared to the control group, the LIPUS group, and the OIGFs group. However, based on the results of the present study, this conclusion cannot be made.

Next, root resorption lacunae depths, lengths, and volumes were measured on each tooth root in every treatment group (Figure 4-9; Figure 4-10; Figure 4-11). The results of the present study show that the mean lacunae depth in each of the treatment groups was significantly less compared to the mean depth in the control group. Root resorption lacunae depth is related to the severity of root resorption. Since the second and third degrees of severity of root resorption involve resorption of dentin and not only cementum as in the first degree, it can be suggested that severity of root resorption is directly related to resorption depth. Resorption that proceeds into at least the outer layers of the dentin may or may not be repaired. Because lacunae depth in the control group was significantly greater compared to each treatment, the resorption that occurred in these tooth roots was significantly more severe than in the treatment groups.

The results of this study also show that the group that received both LIPUS treatment and injection of OIGFs had an even greater decrease in lacunae depth compared to the other treatment groups. Although there was no significant difference between the OIGFs+LIPUS

group's lacunae depth compared to the other treatment groups, the p-value is this group was less than 0.01, whereas the p-value between the other treatment groups and the control group was only less than 0.05. This may represent a greater effect of the combination treatment group on repair of OIRR compared to each of the treatment modalities employed alone.

Lacunae length was also measured for each root in every treatment and control group (Figure 4-10). The results from this analysis show that there was no significant difference between the lacunae lengths in each of the treatment groups compared to the control group. However, although it was statistically non-significant, the control group contained the longest lacunae. The length of lacunae may show less importance in reference to the severity of root resorption.

Finally, lacunae volume was also measured for each lacuna on the surface of each tooth root in every treatment and control group (Figure 4-11). Lacunae volume incorporates both lacunae length and depth, however, it more accurately demonstrates severity of resorption and is more commonly used in other research studies. The present study demonstrates that lacunae volume was statistically significantly greater in the control group compared to each of the treatment groups. These results are similar to those of the lacunae depth measurements, however the treatment groups have even less lacunae volume than lacunae depth when compared to the control. This is based on the p-value. The LIPUS group had a p-value of less than 0.0001, the BMP2 group and the OIGFs+LIPUS group had p-values of less than 0.001, and the OIGFs group had a p-value of less than 0.05. Although these groups were significantly less in lacunae volume compared to the control group, each of these treatment groups was not significantly different from one another.

A previous study that measured volume of resorption lacunae in tooth roots in dogs and compared these measurements between roots that received LIPUS treatment during tooth movement and those that did not receive any treatment during tooth movement also found similar results (Al-Daghreer et al., 2014). In this study the total volume of resorption was significantly lesser in the LIPUS group compared to the control group ( $p < 0.01$ ). This supports the findings in the present study.

Based on these results of  $\mu$ CT analysis of root resorption, it is evident that LIPUS, OIGFs, BMP2, and OIGFs+LIPUS treatments had an effect in the reparative process on OIRR. LIPUS has been shown to have a reparative effect based on its anabolic result on cementoblasts (Dalla-Bona et al., 2008; Inubushi et al., 2008; Dalla-Bona et al., 2006; Rego et al., 2010), which are considered to be the main reparative cell line in the case of root resorption (Jimenez-Pellegrin and Arana-Chavez, 2007; Gotz et al., 2006; Casa et al., 2006). In these studies, LIPUS upregulated proteins including ALP, therefore stimulating mineralization by these cells. This may have led to the reparative effect of LIPUS on cementoblasts in the present study, which resulted in less lacunae depth and volume in the LIPUS and OIGFs+LIPUS groups compared to the control group. Since OIGFs have stem cell properties (Figure 4-1) and also have increased ALP activity (Figure 4-2), LIPUS stimulation may have also upregulated ALP activity in these osteogenic cells and may have induced their differentiation into cementoblast-like cells because of their possible multipotent potential.

In a clinical study, LIPUS was reported to have minimized root resorption by means of accelerating healing of resorption by reparative cementum when LIPUS was applied simultaneously with orthodontic tooth movement (El-Bialy et al., 2004). In another study,

LIPUS was shown to regulate osteoclast differentiation through the OPG/RANKL ratio (Liu et al., 2012). This initiated the reparative effect of LIPUS on OIRR, since osteoclast activity decreased due to its application.

Gingival cells have been reported to inhibit osteoclast activity (de Vries et al., 2006). This inhibition is a property of osteoblasts. It may be possible that gingival cells contain many similar properties as osteoblasts, therefore may aid in the reparative process of OIRR as osteoblasts would. This may have been evident in the present study since the OIGFs group and the OIGFs+LIPUS group each had significantly less root resorption depth and volume compared to the control.

#### **V.IV. Limitations**

The present study suggests that LIPUS, OIGFs, and the combination of both LIPUS and OIGFs may be promising treatments for repair of OIRR. However, there are many limitations to the present study, which prevents it from direct translation into clinical research. When obtaining and characterizing the types of cells used in the present study, it would have more reliable to use a homogeneous population of gingival cells, possibly mesenchymal stem cells. This study shows that this population may have consisted of variety of different types of cells. This may have caused a decrease in the effect of the cells in repairing OIRR that would have otherwise been evident if a pure population was employed.

The present study showed varying results of the effect of each type of treatment on OIRR through histomorphometric analysis measuring the thickness of PDL tissues, including PDL

and cementum. Since these results do not show definitive conclusions, only suggestive conclusions, it cannot be concluded that treatment modalities had definite reparative effect on root resorption. The present study simply measured the PDL tissues (PDL and cementum) on compression and tension sides of the tooth root because bodily tooth movement in the mesial-distal direction mainly affects compression and tension sides of the root. Measurements on the buccal and lingual sides of the root would have provided additional information for the present study. Also, there may have also been a greater significant difference between treatments and control group if cellular and acellular cementum was measured and compared separately, since they vary between root levels.

Also, it is important to note that the measurements in the present study were only performed once. To ensure reproducibility, these measurements of histomorphometric and  $\mu$ CT would need to be performed again either by the same researcher or another researcher using an intra-reliability test or inter-reliability test, respectively.

Since the present study only considered histological analyses (histomorphometric and  $\mu$ CT), greater details on protein and gene expression levels in each group using RT-PCR and immunohistochemistry would have been provided in order to accurately determine the full effect of LIPUS and/or OIGFs on OIRR. Also, looking at these treatment modalities' effects on inflammatory mediators such as IL-1, IL-6, and TNF-alpha in OIRR could aid in assessing their effects on the inflammatory process.

Finally, this study was unable to mark and track OIGFs that were injection into the PDL. Using long-term cell markers would allow the localization of the injected cells to be determined, supporting the assumption that they were incorporated into the PDL and actually had an effect

in the reparative process. The length of the study while using cell markers would have to be considered. To translate this research into clinical research and then clinical treatment of OIRR, the study would have to be increased in duration in order to make it clinically realistic. However, currently there are no cell markers that are available for a length of study as the present one, or are there any for a study with a longer, more clinically-relevant time frame.

### **V.V. Future work**

Based on the results of the present study and the limitations of this work, there are recommendations available for future work in order to further reveal and demonstrate the effect of LIPUS and OIGFs on repair of OIRR. A future study in which a more homogeneous population of mesenchymal stem cells derived from the gingiva would show more reliable and definitive evidences that GFs, osteogenically-induced or not, do have an effect on repair of root resorption. Tracking these stem cells using cell markers would allow localization of these cells to be determined after their incorporation into the PDL. It may also be interesting to look at different concentrations of cells injected as opposed to one concentration used in the current study.

Another suggestion for future studies on the current topic would be to employ another control group that did not receive orthodontic tooth movement. Since the current study involved manipulation to each treatment and control group, it would be more helpful to include a group that did not receive any manipulation in order to correctly compare between treatments and negative and positive controls.

It is also important to consider the topic of prevention of OIRR. A further suggestion for future work would include the use of LIPUS and/or OIGFs during orthodontic tooth movement application instead of post-movement. Since OIRR involves an inflammatory process, anti-inflammatory properties of LIPUS and suppressive activity of MSCs should be explored. A report on the immunosuppressive properties of MSCs revealed that these cells, in addition to their regenerative properties, hold an immunoregulatory capacity due to their low expression of MHC-II and direct cell-to-cell interactions (De Miguel et al., 2012). This future study may show greater statistical significance in prevention of OIRR than the current study that examined the repair of OIRR.

In order to continue such research towards clinical trials, a pre-clinical *in vitro* study is required. This study would need to determine the effect of LIPUS and OIGFs on human tooth roots that have been subject to orthodontic tooth movement. Tracking these cells would be required, however, would only be limited to observing these cells in the root cementum, since the PDL and bone of the human periodontal tissues could not be available in an *in vitro* study because of ethical reasons. Also, determining whether or not osteogenically inducing GFs is required for OIRR repair would be helpful.

## **V.VI. Conclusions**

The present study showed the effect of LIPUS and OIGFs, alone or in combination, on repair of OIRR. Histomorphometric analyses suggest that LIPUS and OIGFs+LIPUS treatments may have been effective at increasing cementum thickness near the apex of the tooth root on the compression side. Further results of the study show that none of the treatments had an effect on

the width of the PDL, however, LIPUS, OIGFs and the combination of the two treatments may have been effective at increasing PDL cellularity on the tension side of the root. The combination of LIPUS and OIGFs did not have a greater reparative effect on PDL tissues compared to each treatment used alone.

Using  $\mu$ CT analysis of the root, it was shown that there was no effect of any of the treatments on root length or root resorption lacunae length. Measurements of root resorption depth and volume show that there may have been a significant effect of LIPUS, OIGFs, and OIGFs+LIPUS on repair of OIRR since these treatments decreased these two measurements when compared to the control group. However, the effect of the combination of OIGFs and LIPUS was not significantly greater than each treatment alone.

Although additional studies are required in order to determine the full reparative effect of these treatments, the present study may possibly suggest that LIPUS and OIGFs, used alone or in combination, could be a future technique for repair of orthodontically induced root resorption.

## References

1. Abramovich A. Effect of ultrasound on the tibia of the young rat. J Dent Res 1970; 49: 1182.
2. Al-Daghreer S, Doschak M, Sloan A, Major P, Heo G, Scurtescu C, Tsui Y, El-Bialy T. Effect of low-intensity pulsed ultrasound on orthodontically induced root resorption in beagle dogs. Ultrasound in Med. & Biol. 2014; 40: 1187-1196.
3. Azuma Y, Ito M, Harada Y, Takagi H, Ohta T, Jingushi S. Low-intensity pulsed ultrasound accelerates rat femoral fracture healing by acting on the various cellular reactions in the fracture callus. J Bone Miner Res. 2001; 16: 671-680.
4. Bosshardt D, Selvig K. Dental cementum: the dynamic tissue covering of the root. Periodontology 2000. 1997; 13: 41-75.
5. Brezniak N, Wasserstein A. Orthodontically induced inflammatory root resorption. Part I: The basic science aspects. Angle Orthodontist. 2002; 72: 175-179.
6. Casa M, Faltin R, Faltin K, Arana-Chavez V. Root resorption on torqued human premolars shown by tartrate-resistant acid phosphatase histochemistry and transmission electron microscopy. Angle Orthodontist. 2006; 76: 1015-1021.
7. Chapman I, MacNally N, Tucker S. Ultrasound-induced changes in rates of influx and efflux of potassium ions in rat thymocytes *in vitro*. Ultrasound med Biol. 1980; 6: 47-58.
8. Chen Y, Wang C, Yang K, Chang P, Huang H, Huang Y, Sun Y, Wang F. Pertussis toxin-sensitive Gai protein and ERK dependent pathways mediate ultrasound

- promotion of osteogenic transcription in human osteoblasts. *FEBS Lett.* 2003; 554: 154-158.
9. Cheung W, Chow S, Sun M, Qin L, Leung K. Low-intensity pulsed ultrasound accelerated callus formation, angiogenesis and callus remodeling in osteoporotic fracture healing. *Ultrasound Med Biol.* 2011; 37: 231-238.
  10. Claes L, Willie B. The enhancement of bone regeneration by ultrasound. *Prog Biophys Mol Biol.* 2007; 93: 384-398.
  11. Cwyk F, Scat-Pierre F, Tronstad L. Endodontic implications of orthodontic tooth movement. *J Dent Res.* 1984; 63: Abstract 1039.
  12. Dalla-Bona D, Tanaka E, Oka H, Yamano E, Kawai N, Miyauchi M, Takata T, Tanne K. Effects of ultrasound on cementoblast metabolism *in vitro*. *Ultrasound in Medicine and Biology.* 2006; 32: 943-948.
  13. Dalla-Bona D, Tanaka E, Inubushi T, Oka H, Ohta A, Okada H, Miyauchi M, Takata T, Tanne K. Cultured cementoblast stimulation by low- and high-intensity ultrasound. *Arch Oral Biol.* 2008; 53: 318-323.
  14. De Miguel P, Fuentes-Julian S, Blazquez-Martinez A, Pascual C, Aller M, Arias J, Arnalich-Montiel F. Immunosuppressive properties of mesenchymal stem cells: advances and applications. *Current Molecular Medicine.* 2012; 12(5): 574-591.
  15. De Vasconcellos L, Ricardo L, Balducci I, de Vasconcellos L, Carvalho Y. Histological analysis of effects of 24% EDTA gel for nonsurgical treatment of periodontal tissues. *J Oral Sci.* 2006; 48: 207-214.
  16. De Vries TJ, Schoenmaker T, Wattanaroonwong N, van den Hoonaard M, Nieuwenhuijse A, Beertsen W, Everts V. Gingival fibroblasts are better at inhibiting

- osteoclast formation than periodontal ligament fibroblasts. *J Cell Biochem.* 2006; 98(2): 370-382.
17. Doan N, Reher P, Meghji S, Harris M. *In vitro* effects of therapeutic ultrasound on cell proliferation, protein synthesis, and cytokine production by human fibroblasts, osteoblasts, and monocytes. *J Oral Maxillofac Surg.* 1999; 57: 409–419.
18. Doğan A, Ozdemir A, Kubar A, Oygür T. Assessment of periodontal healing by seeding of fibroblast-like cells derived from regenerated periodontal ligament in artificial furcation defects in a dog: a pilot study. *Tissue Eng.* 2002; 8: 273-282.
19. Dominici M, Le Blanc K, Mueller I, Slaper-Cortenbach I, Marini F, Krause D, Deans R, Keating A, Prockop D, Horwitz E. Minimal criteria for defining multipotent mesenchymal stromal cells. The International Society for Cellular Therapy position statement. *Cytotherapy.* 2006; 8(4): 315-317.
20. Dyson M, Pond J, Joseph J, Warwick R. The stimulation of tissue regeneration by means of ultrasound. *Clin Sci.* 1968; 35: 273-285.
21. Dyson M, Brookes M. Stimulation of bone repair by ultrasound. *Ultrasound Med Biol.* 1983; 2: 61-66.
22. Dyson M. Therapeutic applications of ultrasound. In: Nyborg WL, Ziskin MC, editors. *Biological effects of ultrasound.* New York: Churchill Livingstone; 1985. p. 121-133.
23. El-Bialy T, Royston T, Magin R, Evans C, Frizzell L. The effect of pulsed ultrasound on mandibular distraction. *Ann Biomed Eng.* 2002; 30: 1251-1261.
24. El-Bialy T, El-Shamy I, Graber TM. Repair of orthodontically induced root resorption by ultrasound in humans. *Am J Orthod Dentofacial Orthop.* 2004; 126: 186–193.

25. El-Bialy T, Elgazzar R, Megahed E, Royston T. Effects of ultrasound modes on mandibular osteodistraktion. *J Dent Res.* 2008; 87: 953-957.
26. El-Bialy T, Alhadlaq A, Wong B, Kucharski C. Ultrasound effect on neural differentiation of gingival stem/progenitor cells. *Ann Biomed Eng.* 2014; 42(7): 1406-1412.
27. Erdogan O, Esen E, Ustün Y, Kürkçü M, Akova T, Gönlüşen G, Uysal H, Cevlik F. Effects of low-intensity pulsed ultrasound on healing of mandibular fractures: an experimental study in rabbits. *J Oral Maxillofac Surg.* 2006; 64: 180-188.
28. Garrett S. Periodontal regeneration around natural teeth. *Ann Periodontol.* 1996; 1: 621-666.
29. Gotz W, Kunert D, Zhang D, Kawarizadeh A, Lossdorfer S, Jager A. Insulin-like growth factor system components in the periodontium during tooth root resorption and early repair processes in the rat. *Eur J Oral Sci.* 2006; 114: 318-327.
30. Harle J, Salih V, Knowles J, Mayia F, Olsen I. Effects of therapeutic ultrasound on osteoblast gene expression. *J Mater Sci Mater Med.* 2001; 12: 1001-1004.
31. Harle J, Salih V, Mayia F, Knowles J, Olsen I. Effects of ultrasound on the growth and function of bone and periodontal ligament cells *in vitro*. *Ultrasound Med Biol.* 2001; 27: 579-586.
32. Harry M, Sims M. Root resorption in bicuspid intrusion. A scanning electron microscope study. *Angle Orthod.* 1982; 52: 235-258.
33. Heckman J, Ryaby J, McCabe J, Frey J, Kilcoyne R. Acceleration of tibial fracturehealing by non-invasive, low-intensity pulsed ultrasound. *J Bone Joint Surg Am.* 1994; 76: 26-34.

34. Horwitz E, Le B, Dominici M. Clarification of nomenclature for MSC: the International Society for Cellular Therapy position statement. *Cytotherapy*. 2005; 7: 393-395.
35. Hu B, Zhang Y, Zhou J, Li J, Deng F, Wang Z, Song J. Low-intensity pulsed ultrasound stimulation facilitates osteogenic differentiation of human periodontal ligament cells. *PLoS One*. 2014; 9(4): e95168.
36. Iashchenko L, Ostapiak Z, Semenov VL. The humoral mechanisms of the action of ultrasound in inflammatory lung diseases (an experimental study). *Vopr Kurortol Fizioter Lech Fiz Kult*. 1994: 20-22.
37. Ikai H, Tamura T, Watanabe T, Ito M, Sugaya A, Iwabuchi S, Mikuni-Takagaki Y, Deguchi S. Low-intensity pulsed ultrasound accelerates periodontal wound healing after flap surgery. *J Periodontal Res*. 2008; 43(2): 212-216.
38. Ikeda E, Morita R, Nakao K, Ishida K, Nakamura T, Takano-Yamamoto T, Ogawa M, Mizuno M, Kasuheckmangai S, Tsuiji T. Fully functional bioengineered tooth replacement as an organ replacement therapy. *Proc Nat Acad Sci, USA*. 2009; 106: 13475-13780.
39. Inubushi T, Tanaka E, Rego EB, Kitagawa M, Kawazoe A, Ohta A, Okada H, Koolstra JH, Miyauchi M, Takata T, Tanne K. Effects of ultrasound on the proliferation and differentiation of cementoblast lineage cells. *Journal of Periodontology*. 2008; 79: 1984-1990.
40. Iwabuchi Y, Tanimoto K, Tanne Y, Inubushi T, Kamiya T, Huang Y, Kunimatsu R, Hirose N, Yoshioka M, Mitsuyoshi T, Tanaka E, Tanne K. Effects of low-intensity pulsed ultrasound on the expression of cyclooxygenase-2 in mandibular condylar chondrocytes. *J Oral Facial Pain Headache*. 2014; 28: 261-268.

41. Jimenez-Pellegrin C, Arana-Chavez V. Root resorption repair in mandibular first premolars after rotation. A transmission electron microscopy analysis combined with immunolabeling of osteopontin. *Am J Orthod Dentofacial Orthop.* 2007; 132: 230-236.
42. Kanbe K, Inoue K, Inoue Y, Chen Q. Inducement of mitogen-activated protein kinases in frozen shoulders. *J Orthop Sci.* 2009; 14: 56-61.
43. Kawaguchi H, Hirachi A, Hasegawa N, Iwata T, Hamaguchi H, Shiba H, Takata T, Kato Y, Kurihara H. Enhancement of periodontal tissue regeneration by transplantation of bone marrow mesenchymal stem cells. *J Periodontol.* 2004; 75: 1281–1287.
44. Kim S, Kim K, Seo B, Koo K, Kim T, Seol Y, Ku Y, Rhyu I, Chung C, Lee Y. Alveolar bone regeneration by transplantation of periodontal ligament stem cells and bone marrow stem cells in a canine peri-implant defect model: a pilot study. *J Periodontol.* 2009; 80: 1815-1823.
45. Kokubu T, Matsui N, Fujioka H, Tsunoda M, Mizuno K. Low intensity pulsed ultrasound exposure increases prostaglandin E2 production via the induction of cyclooxygenase-2 mRNA in mouse osteoblasts. *Biochem Biophys Res Commun.* 1999; 256: 284-287.
46. Krieger E, Hornikel S, Wehrbein H. Age-related changes of fibroblast density in the human periodontal ligament. *Head & Face Medicine.* 2013; 9: 22-25.
47. Lee J, Stavropoulos A, Susin C, Wikesjö U. Periodontal regeneration: focus on growth and differentiation factors. *Dent Clin N Am.* 2010; 54: 93-111.
48. Leung K, Cheung W, Zhang C, Lee K, Lo H. Low intensity pulsed ultrasound stimulates osteogenic activity of human periosteal cells. *Clin.Orthop.* 2004; 418: 253-259.

49. Li F, Wang Z, Du Y, Ma P, Bai J, Wu F, Feng R. Study on therapeutic dosimetry of HIFU ablation tissue. *Sheng Wu Yi Xue Gong Cheng Xue Za Zhi*. 2006; 23: 839-843.
50. Lim K, Kim J, Seonwoo H, Park S, Choung P, Chung J. *In vitro* effects of low-intensity pulsed ultrasound stimulation on the osteogenic differentiation of human alveolar bone-derived mesenchymal stem cells for tooth tissue engineering. *Biomed Res Int* 2013. 2013; 269724.
51. Lin N, Gronthos S, Bartold P. Stem cells and periodontal regeneration. *Aust Dent J*. 2008; 53: 108–121.
52. Liu Z, Xu J, E L, Wang D. Ultrasound enhances the healing of orthodontically induced root resorption in rats. *Angle Orthod*. 2012; 82: 48-55.
53. Maeda H, Tomokiyo A, Fujii S, Wada N, Akamine A. Promise of periodontal ligament stem cells in regeneration of periodontium. *Stem Cell Research & Therapy*. 2011; 2: 33.
54. Maylia E, Nokes L. The use of ultrasonics in orthopaedics—a review. *Technol Health Care* 1999; 7: 1-28.
55. McGuire M, Scheyer E. A randomized, double-blind, placebo-controlled study to determine the safety and efficacy of cultured and expanded autologous fibroblast injections for the treatment of interdental papillary insufficiency associated with the papilla priming procedure. *J Periodontol*. 2007; 78(1): 4–17.
56. Mirabella A, Artun J. Prevalence and severity of apical root resorption of maxillary anterior teeth in adult orthodontic patients. *Eur J Orthod*. 1995; 17: 93-99.

57. Miyaji H, Sugaya T, Ibe K, Ishizuka R, Tokunaga K, Kawanami M. Root surface conditioning with bone morphogenetic protein-2 facilitates cementum-like tissue deposition in beagle dogs. *J Periodont Res.* 2010; 45: 658-663.
58. Mohammadi M, Shokrgozar M, Mofid R. Culture of human gingival fibroblasts on a biodegradable scaffold and evaluation of its effect on attached gingiva: a randomized, controlled pilot study. *J Periodontol.* 2007; 78: 1897–1903.
59. Mostafa N, Scott P, Dederich D, Doschak M, El-Bialy T. Low intensity pulsed ultrasound stimulates osteogenic differentiation of human gingival fibroblasts. *Proc Ann Mtg Can Acoustics Assoc.* 2008; 36: 34–35.
60. Mostafa N, Scott P, Doschak M, Dederich D, El-Bialy T. EMD enhances fibroblast colonization and morphologic changes on root surface. *Ann Mtg Int Assoc Dent Res, Toronto, Canada.* 2008; Abstract 0795.
61. Mostafa N, Uludağ H, Dederich D, Doschak M, El-Bialy T. Anabolic effects of low-intensity pulsed ultrasound on human gingival fibroblasts. *Arch. Oral. Biol.* 2009; 54: 743-748.
62. Mukai S, Ito H, Nakagawa Y, Akiyama H, Miyamoto M, Nakamura T. Transforming growth factor- $\beta$ 1 mediates the effects of low-intensity pulsed ultrasound in chondrocytes. *Ultrasound Med Biol.* 2005; 31: 1713-1721.
63. Nagata K, Nakamura T, Fujihara S, Tanaka E. Ultrasound modulates the inflammatory response and promotes muscle regeneration in injured muscles. *Ann Biomed Eng.* 2013; 41: 1095-1105.
64. Nakamura T, Fujihara S, Katsura T, Yamamoto K, Inubushi T, Tanimoto K et al. Effects of low-intensity pulsed ultrasound on the expression and activity of hyaluronan

- synthase and hyaluronidase in IL-1beta-stimulated synovial cells. *Ann Biomed Eng.* 2010; 38: 3363-3370.
65. Nakamura T, Fujihara S, Yamamoto-Nagata K, Katsura T, Inubushi T, Tanaka E. Low intensity pulsed ultrasound reduces the inflammatory activity of synovitis. *Ann Biomed Eng.* 2011; 39: 2964-2971.
66. Nanci A, Bosshardt D. Structure of periodontal tissues in health and diseases. *Periodontology 2000.* 2006; 40: 11-26.
67. Naruse N, Miyauchi A, Itoman M, Mikuni-Takagaki Y. Distinct anabolic response of osteoblasts to low-intensity pulsed ultrasound. *J Bone Miner Res.* 2003; 18: 360-369.
68. Neve A, Corrado A, Cantatore F. Osteoblast physiology in normal and pathological conditions. *Cell Tissue Res.* 2011; 343: 289-302.
69. Rego E, Inubushi T, Kawazoe A, Tanimoto K, Miyauchi M, Tanaka E et al. Ultrasound stimulation induces PGE2 synthesis promoting cementoblastic differentiation through EP2/EP4 receptor pathway. *Ultrasound in Medicine and Biology.* 2010; 36: 907-915.
70. Ren L, Yang Z, Song J, Wang Z, Deng F, Li W. Involvement of p38 MAPK pathway in low intensity pulsed ultrasound induced osteogenic differentiation of human periodontal ligament cells. *Ultrasonics.* 2013; 53(3): 686-690.
71. Rita F, David E, James L. Tooth resorption. *Quint Int.* 1999; 30: 9-25.
72. Ritchie R, Collin J, Coussios C, Leslie T. Attenuation and de-focusing during high-intensity focused ultrasound therapy through peri-nephric fat. *Ultrasound Med Biol.* 2013; 39: 1885-1793.

73. Sabokbar A, Millett P, Myer B, Rushton N. A rapid, quantitative assay for measuring alkaline phosphatase activity in osteoblastic cells *in vitro*. *Bone and Mineral*. 1994; 27: 57-67.
74. Saito N, Okada T, Horiuchi H, Ota H, Takahashi J, Murakami N, Nawata M, Kojima S, Nozaki K, Takaoka K. Local bone formation by injection of recombinant human bone morphogenetic protein-2 contained in polymer carriers. *Bone*. 2003; 32: 381-386.
75. Saito M, Fujii K, Tanaka T, Soshi S. Effect of low and high intensity pulsed ultrasound on collagen post-translational modifications in MC3T3-E1 osteoblasts. *Calcif Tissue Int*. 2004; 75: 384-395.
76. Sakallioğlu U, Açıkgoz G, Ayas B, Kirtiloğlu T, Sakallioğlu E.: Healing of periodontal defects treated with enamel matrix proteins and root surface conditioning--an experimental study in dogs. *Biomaterials*. 2004; 25(10): 1831-1840.
77. Scheven B, Man J, Millard J, Cooper P, Lea S, Walmsley A, Smith A. VEGF and odontoblast-like cells: stimulation by low frequency ultrasound. *Arch Oral Biol*. 2009; 54: 185-191.
78. Scholzen T, Gerdes J. The Ki-67 protein: from the known and the unknown. *J Cell Physiol*. 2000; 182(3): 311-322.
79. Schumann D, Kujat R, Zellner J, Angele M, Nerlich M, Mayr E, Angele P. Treatment of human mesenchymal stem cells with pulsed low intensity ultrasound enhances the chondrogenic phenotype *in vitro*. *Biorheology*. 2006; 43: 431-443.
80. Seo B, Miura M, Gronthos S, Bartold P, Batouli S, Brahim J, Young M, Robey P, Wang C, Shi S. Investigation of multipotent postnatal stem cells from human periodontal ligament. *Lancet*. 2004; 364: 149–155.

81. Shiraishi R, Masaki C, Toshinaga A, Okinaga T, Nishihara T, Yamanaka N, Nakamoto T, Hosokawa R. The effects of low-intensity pulsed ultrasound exposure on gingival cells. *J Periodontol.* 2001; 82(10): 1498-1503.
82. Silvério K, Benatti B, Casati M, Sallum E, Nociti F. Stem cells: potential therapeutics for periodontal regeneration. *Stem Cell Rev.* 2008; 4: 13-19.
83. Simmons P, Torok-Storb B. Identification of stromal cell precursors in human bone marrow by a novel monoclonal antibody, STRO-1. *Blood.* 1991; 78(1): 55-62.
84. Takeuchi R, Ryo A, Komitsu N, Mikuni-Takagaki Y, Fukui A, Takagi Y, Shiraishi T, Morishita S, Yamazaki Y, Kumagai K, Aoki I, Saito T. Low-intensity pulsed ultrasound activates the phosphatidylinositol 3 kinase/Akt pathway and stimulates the growth of chondrocytes in three-dimensional cultures: a basic science study. *Arthritis Res Ther.* 2008; 10: R77.
85. Tanaka E, Kuroda S, Horiuchi S, Tabata A, El-Bialy T. Low-intensity pulsed ultrasound in dentofacial tissue engineering. *Ann Biomed Eng.* 2015; (Epub ahead of print).
86. Tobita M, Uysal A, Ogawa R, Hyakusoku H, Mizuno H. Periodontal tissue regeneration with adipose-derived stem cells. *Tissue Eng Part A.* 2008; 14: 945–953.
87. Tsai C, Chang W, Liu T. Preliminary studies of duration and intensity of ultrasonic treatments on fracture repair. *Chin J Physiol.* 1992; 35: 21-26.
88. Walker P, Jimenz F, Gerber M, Aroom K, Shah S, Harling M, Gill B, Savitz S, Cox (Jr.) C. Effect of needle diameter and flow rate on rat and human mesenchymal stromal cell characterization and viability. *Tissue Engineering: Part C.* 2010; 16(5): 989-997.

89. Warden S, Bennell K, McMeeken J, Wark J. Acceleration of fresh fracture repair using the soic accelerated fracture healing system (SAFHS): A review. *Calcif Tissue Int.* 2000; 66: 157-163.
90. Wong A, Mostafa N, Uludag H, El-Bialy T. Osteogenic and adipogenic induction potential of human gingival fibroblasts. *Proc Alberta Biomed Eng, Banff, AB.* 2008; [Poster presentation].
91. Yamada Y, Ueda M, Hibi H, Baba S. A novel approach to periodontal tissue regeneration with mesenchymal stem cells and platelet-rich plasma using tissue engineering technology: a clinical case report. *Int J Periodontics Restorative Dent.* 2006; 26: 363–369.
92. Yamamoto T, Domon T, Takahashi S, Suzuki R, Islam M. The fibrillary structure of cement lines on resorbed root surfaces of human teeth. *J Periodont Res.* 2000; 35: 208-213.
93. Yoon J, Roh E, Shin S, Jung N, Song E, Lee D, Han K, Kim J, Kim B, Jeon H, Yoon K. Introducing pulsed low-intensity ultrasound to culturing human umbilical cord-derived mesenchymal stem cells. *Biotechnol.Lett.* 2009; 31(3): 329-335.
94. Young S, Dyson M. The effect of therapeutic ultrasound on angiogenesis. *Ultrasound Med Biol.* 1990; 16: 261-269.
95. Ziskin M. Applications of ultrasound in medicine-comparison with other modalities. In: Repacholi MH, Grandolfo M, Rindi A, editors. *Ultrasound: medical applications, biological effects, and hazard potential.* New York: Plenum Press; 1987. p. 49-59.

**Appendix**

Appendix 1 continued

**CLINICAL SIGNS CHECKLIST**

Animal # D-1

Date: <u>May 12, 08 13:30</u>	Please Circle		Comments
Eating:	<input checked="" type="radio"/> Yes	/ No	
Drinking:	<input checked="" type="radio"/> Yes	/ No	
Able to stand on all 4 legs:	<input checked="" type="radio"/> Yes	/ No	
Able to walk:	<input checked="" type="radio"/> Yes	/ No	
Dehydrated:	Yes /	<input checked="" type="radio"/> No	
Defecating:	Yes /	<input checked="" type="radio"/> No	
Urinating:	<input checked="" type="radio"/> Yes	/ No	
Hunched abdomen:	Yes /	<input checked="" type="radio"/> No	NA
Incision Check:	Yes /	No	NA
Mucous Membrane /Extremities:	(Circle all that apply) Blue / <input checked="" type="radio"/> Pink White		CRT 2
	Cold / <input checked="" type="radio"/> Warm		
Analgesic:	Yes /	<input checked="" type="radio"/> No	Dose: _____ Route: _____ Time: _____

Date: <u>May 12/08 19:00</u>	Please Circle		Comments
Eating:	<input checked="" type="radio"/> Yes	/ No	
Drinking:	<input checked="" type="radio"/> Yes	/ No	
Able to stand on all 4 legs:	<input checked="" type="radio"/> Yes	/ No	
Able to walk:	<input checked="" type="radio"/> Yes	/ No	
Dehydrated:	Yes /	<input checked="" type="radio"/> No	
Defecating:	Yes /	<input checked="" type="radio"/> No	
Urinating:	<input checked="" type="radio"/> Yes	/ No	
Hunched abdomen:	Yes /	No	NA
Incision Check:	Yes /	No	NA
Mucous Membrane /Extremities:	(Circle all that apply) Blue / <input checked="" type="radio"/> Pink White		CRT 2
	Cold / <input checked="" type="radio"/> Warm		
Analgesic:	Yes /	<input checked="" type="radio"/> No	Dose: _____ Route: _____ Time: _____

13FormaCheck of Clinical Signs.doc

Rev. Nov 2001

Appendix 1-1: Clinical signs checklist.

May 12/08 18:00

PAIN ASSESSMENT IN THE DOG  
SCORING SHEET<sup>1</sup>

ANIMAL IDENTIFICATION: D-1  
TECHNICIAN S. de la P. Piquero

ROOM # 7051  
PROTOCOL # 525

PARAMETER ASSESSED SCORE

A: ACTIVITY<sup>2</sup>:

- bright and alert, standing normal gait 0
- stays in corner, slow to move or restless/agitated 1<sup>3</sup>
- reluctant to move even if prodded gently 2<sup>3</sup>
- reluctant to move even if prodded gently **and** depressed, hunched, eyes partly closed 3<sup>3</sup>
- writhing, or staggering, or back twitching (see Flecknell CD - available at HSLAS) 5
- moribund 9

B: HAIRCOAT AND APPEARANCE

- haircoat shiny and smooth, regular grooming behaviour observed 0
- matted, haircoat rough, dry, and stands up scruffily 2
- matted, unkempt, severe bidirection 3

- decreased water intake, skin tents when pinched 1
- inappetence: score 1 for each day of inappetence 1
- 5% loss of pretreatment body weight 2
- 10% loss of pretreatment body weight 4
- 20% loss of pretreatment body weight 8

TOTAL SCORE: 0

INTERPRETATION: 0 - Normal animal  
3 - 4: mild stress/pain. Fluids and analgesia should be provided  
5 - 8: severe stress/pain, veterinary assessment required  
9 unacceptable stress/pain. Immediate euthanasia required

<sup>1</sup> To use this sheet, circle the number that best applies under each parameter. Total the circled numbers to obtain the pain/discomfort score.  
<sup>2</sup> Most accurately assessed under red light conditions  
<sup>3</sup> Add 1 to this score if the rat also vocalizes

Appendix 1-2: Pain Assessment In The Dog Pain Scoring Sheet.